Chulalongkorn University

The Ratchadaphisek Somphot Endowment Fund

Final Report

On

"Treatment of Dye Containing in Textile Wastewater Using TS-1, Ti-MCM-41 and Bismuth Titanate Catalysts"

By

Ms. Sujitra Wongkasemjit

สถาบันวิทยบริการ
จุฬาลงกรณ์มหาวิทยาลัย

September, 2007

Acknowledgements

This research work is financially supported by the Postgraduate Education and Research Program in Petroleum and Petrochemical Technology (ADB) Fund (Thailand) and the Ratchadapisake Sompote Fund, Chulalongkorn University (Thailand). The authors are very thankful to Assistant Professor Manit Nithithanakul and Thanakul Dyeing and Printing Co., Ltd. for providing the waste-water studied in this work

สถาบันวิทยบริการ
จุฬาลงกรณ์มหาวิทยาลัย

Abstract

This research was to study the photocatalytic activity of three different metal oxide catalysts, namely MCM-41, TS-1, and bismuth titanate ($Bi_{12}TiO_{20}$) in the reactive black 5 dye solution and the waste water obtained from a dye industry. These catalysts were synthesized using silatrane, titanium glycolate and bismuth nitrate precursors. The degradation process was first studied in the reactive black 5 dye model. The parameters in this study were pH, amounts of H_2O_2 and Ti-loading in zeolite structure while fixing the organic dye at 40 ppm. At pH3, all three catalysts showed high photocatalytic activity. The higher amount of H_2O_2 resulted in the higher photocalytic activity. The decoloration and the percent of mineralization increased with the higher Ti-content. The carbon reduction reached 79% using MCM-41 as catalyst, 65% for TS-1 and 35% for bismuth titanate, respectively.

In the real wastewater obtained from Thanakul Dyeing And Printing Co., Ltd., it was found that all the three catalysts showed promising activity results. Moreover, in the case of using MCM-41 as catalyst, the carbon reduction reached 16% with respect to the initial carbon content. The results are very satisfying since the catalysts can oxidize non-pretreated-wastewater from industries under a mild condition

สถาบันวิทยบริการ
จุฬาลงกรณ์มหาวิทยาลัย

.

บทคัดย่อ

งานวิจัยนี้ ต้องการศึกษาความว่องไวในการเร่งปฏิกิริยาของโลหะออกไซด์ 3 ชนิด ได้แก่ MCM-41, TS-1 และ บิสมัทไททเนต (bismuth titanate) ในสารละลายที่มีสีย้อมผ้าชนิด รีแอกทีฟ แบลคไฟว์ (Reactive black 5: RB5) และในน้ำเสียที่ได้รับจากโรงงานย้อมผ้า ตัวเร่งปฏิกิริยาทั้งสามชนิดนั้น สังเคราะห์ได้จากสารตั้งต้น ไซลาเทรน ไททาเนียมไกลโคเลต และบิสมัทไนเตรต โดยในขั้นแรกนั้น ได้ทดลองศึกษากับสารละลายที่มีสีย้อม รีแอกทีฟ แบลคไฟว์ ปัจจัยที่ได้ทำการศึกษานั้นแบ่งออกได้เป็น 3 ประเภท ได้แก่ ผลของค่าความเป็นกรด-เบส ปริมาณของไฮโดรเจนเปอร์ออกไซด์ และ ปริมาณของไทเทเนียมในโครงสร้างของซีโอไลท์ ในขั้นตอนกระบวนการนั้น ทำการละลายให้ได้ความเข้มข้นของสีเท่ากับ 40 มิลลิกรัมต่อลิตร พบว่า ตัวเร่งปฏิกิริยาทั้งสามชนิด เร่งปฏิกิริยาการสลายตัวของสีได้ดีที่สภาวะเป็นกรด และดีที่สุดเมื่อ ค่าความเป็นกรดเท่ากับ 3 เมื่อปริมาณของไฮโดรเจนเปอร์ออกไซด์เพิ่มมากขึ้น ปฏิกิริยาเกิดได้ดีขึ้น และเมื่อปริมาณของไทเทเนียมเพิ่มมากขึ้น อัตราการสลายโครงสร้างของสีทำได้ดีขึ้นตามลำดับ โมเลกุลของสีถูกสลายไปเป็นคาร์บอนไดออกไซด์ ได้มากถึง 79 เปอร์เซ็นต์ เมื่อใช้ MCM-41 เป็นตัวเร่งปฏิกิริยา และ65 เปอร์เซ็นต์เมื่อใช้ TS-1 เป็นตัวเร่งปฏิกิริยา ขณะที่บิสมัตไททาเนตสามารถเร่งการสลายตัวของสารอินทรีย์ให้เป็นคาร์บอนไดออกไซด์ได้เพียง 35 เปอร์เซ็นต์

น้ำเสียจากโรงงานอุตสาหกรรม Thanakul Dyeing And Printing Co., Ltd.ที่ยังไม่ได้ทำการบำบัด ได้ถูกนำมาศึกษาถึงความเป็นไปได้ในการประยุกต์ จากผลการทดลองพบว่า ตัวเร่งปฏิกิริยาทั้งสามให้ผลที่ดี นอกจากนี้ ในกรณีของตัวเร่งปฏิกิริยา Ti-MCM-41 สามารถลดปริมาณคาร์บอนในน้ำเสียได้มากถึง 16 เปอร์เซ็นต์ ซึ่งจากผลการทดลองที่ได้นี้ นับว่าประสบความสำเร็จ เนื่องจากสามารถบำบัดน้ำเสียที่ยังไม่ได้ผ่านการบำบัดมาก่อน ภายใต้สภาวะที่ไม่รุนแรง

TABLE CONTENT

Page

List of Figures

Page

List of Tables

สถาบันวิทยบริการ
จุฬาลงกรณ์มหาวิทยาลัย

Introduction

Azo dyes constitute the largest and the most important class of commercial dyes in wastewater. They are mostly non-biodegradable and resistant to destruction by conventional wastewater treatments[1]. The discharge of highly colored wastewater into the ecosystem involves environmental problems like aesthetic pollution (even a small amount of dye is clearly apparent), and perturbation of aquatic life[2].

Recent studies indicated that toxic and refractory organic compounds including dyes in wastewater can be destroyed by the most advanced oxidation processes (AOPs)[3-5]. Photocatalytic degradation process (UV/TiO_2) as one of the AOPs is receiving increasing attention because of the low cost, relatively high chemical stability of the catalyst and possibility of using sunlight as the source of irradiation[6]. Moreover, photocatalysis does not require expensive oxidants and can be carried out at mild temperature and pressure. TiO_2 is known to be the most active photocatalyst for organic oxidation[8]. However, there are certain limitations of using bare TiO_2 in photocatalytic reactors. For example, due to smaller size (about 4-30 nm) TiO_2 aggregates rapidly in a suspension, loosing its effective surface area as well as the catalytic efficiency. Being non-porous, TiO_2 exhibits low adsorption ability of pollutants[9]. Therefore, putting titanium onto high surface area of silica, as Ti-MCM-41, or putting within the zeolite cavity or the zeolite framework, as in titanium silicalite (TS-1), may have advantages because zeolites have nanoscale pores, high adsorption capacities and ion-exchange capacities[10-12].

The development of titanium-substituted derivatives of the mesoporous molecular sieves MCM-41 was also prepared by post-synthetic methods[13], using Ti-butoxide or titanocene grafting without destroying the mesopore structure. Ti-substituted mesoporous derivatives prepared by both hydrothermal and post-synthetic methods were catalytically active for the selective oxidation of 2,6-DTBP with H_2O_2. Modified Ti-MCM-41 samples were efficient catalysts in the epoxidation and oxidative cyclization using tert-butyl hydroperoxide (TBHP) as oxidant under mild liquid phase reaction conditions[14]. The oxidation activity increases four- to five folds by using TBHP as oxidant over that seen when using aqueous H_2O_2.

TS-1 has become one of increasing interests due to a variety of important applications. The presence of Ti atoms occupying framework position in the zeolite lattice is responsible for the remarkable catalytic properties for a broad range of oxidations with hydrogen peroxide. The isolation of tetrahedrally coordinated Ti atoms in silica correlated with the activity and selectivity of alkane epoxidation reaction, suggesting that those atoms were the active sities for oxidation. The method of synthesis, which affected to the degree of homogeneity of component mixing, played a crucial role in determining the surface character of the final catalytic materials[15].

Another interesting catalyst is bismuth titanate ($Bi_{12}TiO_{20}$) since it is reported that this material has high photocatalytic activity for decoloration of methyl orange[16]. The $Bi_{12}TiO_{20}$ crystal belongs to a family of sillenite compounds with the general formula Bi_2MO_{20} where M represents a tetravalent ion or a combination of ions, which gives an average charge of 4+. The framework of $Bi_{12}TiO_{20}$ crystal structure is formed by Bi–O polyhedra, where Bi ions are coordinated with five oxygen ions that form an octahedral arrangement together with the stereochemically active $6s^2$ lone electron pair of Bi^{3+}. A Bi-O polyhedron network connects to the geometrically regular TiO_4 tetrahedra. Each of the tetrahedra is formed by four oxygen anions while the Ti cation occupies the tetrahedral interstice[17].

Therefore, in this research, we are comparing photocatalytic activities of these three catalysts, viz. Ti-MCM-41, TS-1 and $Bi_{12}TiO_{20}$, in dye-degradation process, concerning both of decoloration and minerization of reactive black 5 dyes used as a model. Effects of the solution acidity and the concentration of H_2O_2 are studied. To observe the effect of Ti content in the MCM-41 and TS-1 zeolite structures, different %Ti loadings and Si/Ti ratios will also be investigated. The suitable conditions will be applied to study the degradation process of waste water samples from industry.

Methodology

Part I Catalyst preparation

Ti-MCM-41[18], TS-1[19] and bismuth titanate[20] catalysts were synthesized following the previous works and using our homemade moisture stable silatrane[21]and titanium glycolate precursors[22].

1. Ti-MCM-41 Synthesis

Ti-MCM-41 was followed the method described in ref. 18. Various ratios of silatrane and titanium glycolate precursors in the range of 1-5 % Ti were studied by adding into a solution containing 0.5 mol CTAB, 0.001 mol NaOH, 0.014 mol TEA and 0.36 mol of water. The mixture was stirred for 3 h to obtain crude product which was purified by washing with deionized water to result in white solid. The white solid was dried at room temperature, calcined at 550°C to remove all organic components, resulting in mesoporous Ti-MCM-41.

2. TS-1 zeolite synthesis

Hydrothermal syntheses were carried out using a sample mixture containing initial molar composition of $xSiO_2$:$yTiO_2$:0.31TPA^+:0.4NaOH: 114H_2O (where x:y = 100, 50, 33, 25, 20 and 12) and microwave irradiation. The mixture was aged at room temperature for 110 h and heated in a microwave at 150ºC for various reaction times, depending on the Ti loading; the higher the Ti-loading, the longer the reaction time, as discussed in ref. 19. Hydrothermal treatment by microwave heating technique was conducted on ETOH SEL, Milestone Microwave Laboratory System (Spec 2500W and 2450MHz). Samples were heated in a Teflon tube. The TS-1 zeolite product was washed several times with distilled water, dried at 60 ºC overnight and calcined at 550 ºC for 2 h at a heating rate of 0.5 ºC/min[19].

3. Bismuth titanate synthesis

Bismuth (III) nitrate pentahydrate was dissolved in nitric acid, and the stoichiometric amount of titanium glycolate was added to the solution with vigorously stirring until the mixture turned clear. The pH of the mixture was adjusted to 5 using 0.1 M nitric acid and 0.1 M ammonium hydroxide. After stirring for 1 h, the mixture was centrifuged at 10,000 rps to separate the precipitate out followed by washing with

water until the filtrate became neutral. The white solid obtained was dried at 60ºC and then calcined at 600ºC for 3 h using a heating rate of 1ºC /min[20].

FTIR spectra were measured on a Thermo Nicolet, Nexus 670 by mixing sample powder with KBr to make a pellet. The crystallographic phase of the products, Ti-MCM-41, TS-1 and $Bi_{12}TiO_{20}$, were characterized using a Rigaku X-ray diffractometer at a scanning speed of 5.0°/s using CuK∝ as source. The working range was 2θ = 0-20 for Ti-MCM-41, 20–60 for TS-1 and $Bi_{12}TiO_{20}$. UV–visible measurement was performed on a Shimadzu UV-2550 with the ISR-2200 Integrating sphere attachment using $BaSO_4$ as a reference. Diffuse reflectance ultraviolet spectroscopy was obtained on a Shimatzu UV-2550 spectrometer. The reflectance output was converted using Kubelka–Munk algorithm. Surface area of the catalysts was determined using Quantasorb JR (Autosorb-1) and BET method.

Part II Activity Testing

1. Using reactive black 5 as a model

The photocatalytic reactions were carried out in a 500 ml batch reactor (Vt =600 ml, Ø=14 cm) equipped with a cooling water jacket to control the temperature at 25ºC. The lamp was vertically immersed in the suspension and illuminated using a commercial 6 W UV lamp (Hg Philip; emission 320-400 nm). Reactive black 5 (RB5) was added into the continuously, magnetically stirred mixture solution at a concentration of 40 ppm, followed by Ti-MCM-41, bismuth titanate or TS-1 zeolite at Si/Ti molar ratios of 100, 50, 33, 25, 20 and 12. The adsorption/degradation equilibrium of the suspensions was established by magnetically stirring in the dark for 60 minutes, prior to irradiation. The concentration of catalyst was fixed at 0.5 g/l using various amounts of H_2O_2 (10, 20, 30 mM/l). The samples were taken out, filtered and then analyzed to determine the concentration of RB5 using Shimadzu UV-240 spectrophotometer at 590 nm which is the maximum absorbance of the reactive black 5 dyes and the total organic content (TOC) using Shimadzu TOC-VC to SH Analyzer.

2. Using industrial waste water

In order to adjust the optimum concentration of waste water from industry the waste water concentration was determined using UV-Vis spectroscopy at 616 nm and TOC analyzer. The stock solution was diluted until the TOC value obtained was around two times higher than that of RB5. The amount of H_2O_2 and catalyst used in this system were also adjusted in proportion with the RB5 system.

Results and Discussion

Characterization of Catalysts

1. Ti-MCM-41

Ti-MCM-41 was synthesized via the sol-gel process to obtain white powder. DRUV used to determine the presence of framework and extra-framework of titanium species shows tetrahedral coordinated species at λ = 200-230 nm, see fig. 1. They are in good agreement with Chatterjee, *et al*. in 2002 and Marchese, *et al*. in 1997[23-24]. When %Ti increased, the DR-UV peak was broader and showed a shoulder at λ = 280 nm, referring to partially polymerized Ti species, as discussed by Thanabodeekij, *et al.* in 2005. The calcined products at various %Ti contents showed a well-resolved pattern of hexagonal mesostructure, as shown in fig. 2. In the figure, XRD spectra give only hk0 reflections and no reflections at diffraction angles larger than 6 degree 2θ were observed. The three-peak positions of 100, 110 and 200 reflections are from long-range structural order of hexagonal arrays. In addition, the considerably good intensity still maintains even % loaded Ti increases. The discovered tendency is similar to the results reported in the reference[18]. The main reason for this remarkable result probably comes from our extraordinary precursors having highly pure and moisture stable properties.

Nitrogen physisorption probes the textural properties of materials, such as, surface area, pore size and pore volume. The BET surface area, pore size and pore volume of Ti-MCM-41 are summarized in Table 1. The result corresponds to a decrease in pore wall thickness of the crystallite sample and indicates that the titanium substituted MCM-41 could be crystallized without decreasing mesoporous size via our normal synthesis process[18]. Surprisingly, the amount of Ti loading onto MCM-41 via

the sol-gel process did not significantly affect to the BET surface area and the pore size.

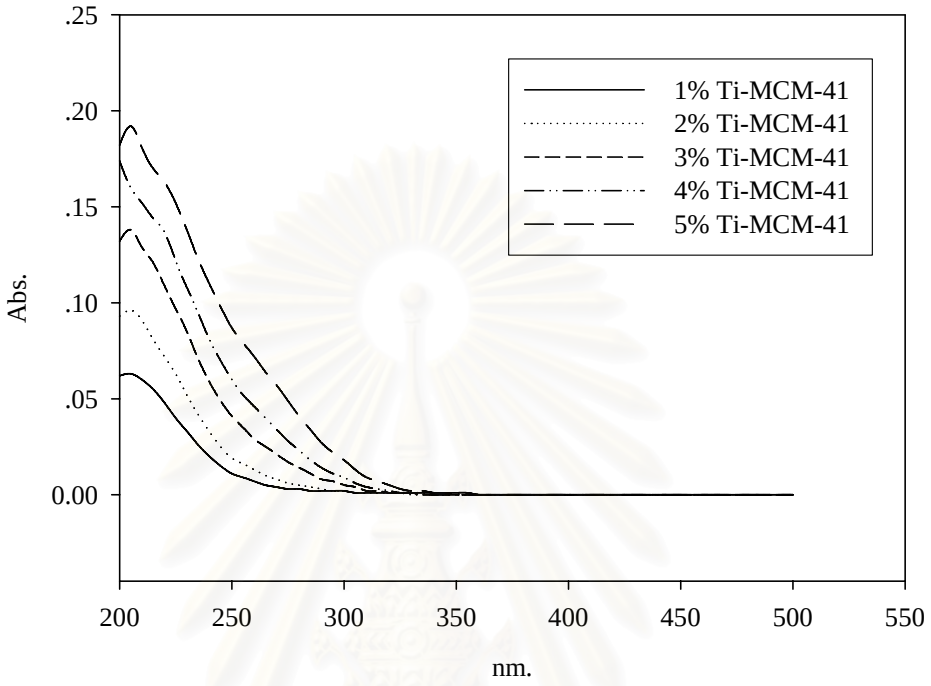

Figure 1 DR-UV results of various Ti-MCM-41 catalysts

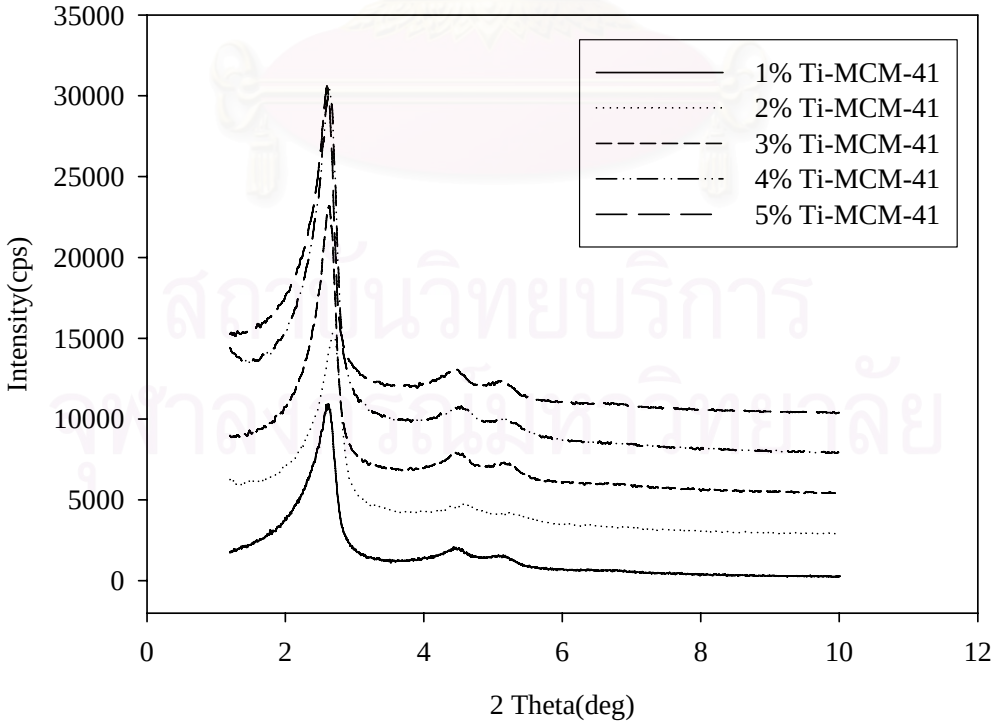

Figure 2 XRD results of various Ti-MCM-41 catalysts

Table 1 BET analysis of Ti-MCM-41 synthesized at different Ti loadings

Catalyst	BET Surface Area (m^2/g)	Pore Volume (cc/g)	Average Pore Size (nm)
1% Ti-MCM-41	1299	0.8265	2.545
2% Ti-MCM-41	1333	0.8570	2.571
3% Ti-MCM-41	1276	0.7457	2.338
4% Ti-MCM-41	1451	0.9060	2.498
5% Ti-MCM-41	1187	0.8200	2.764

2. TS-1 zeolite

The presence of Ti atom in TS-1 can be obtained from the FT-IR band at 960 cm^{-1}, asymmetric stretching mode of Si-O-Ti groups, which is considered as a "fingerprint" for framework Ti atoms in tetrahedral or nearly tetrahedral coordination as shown in fig. 3. The intensity of this peak is proportional to the Ti^{+4} contents[25].

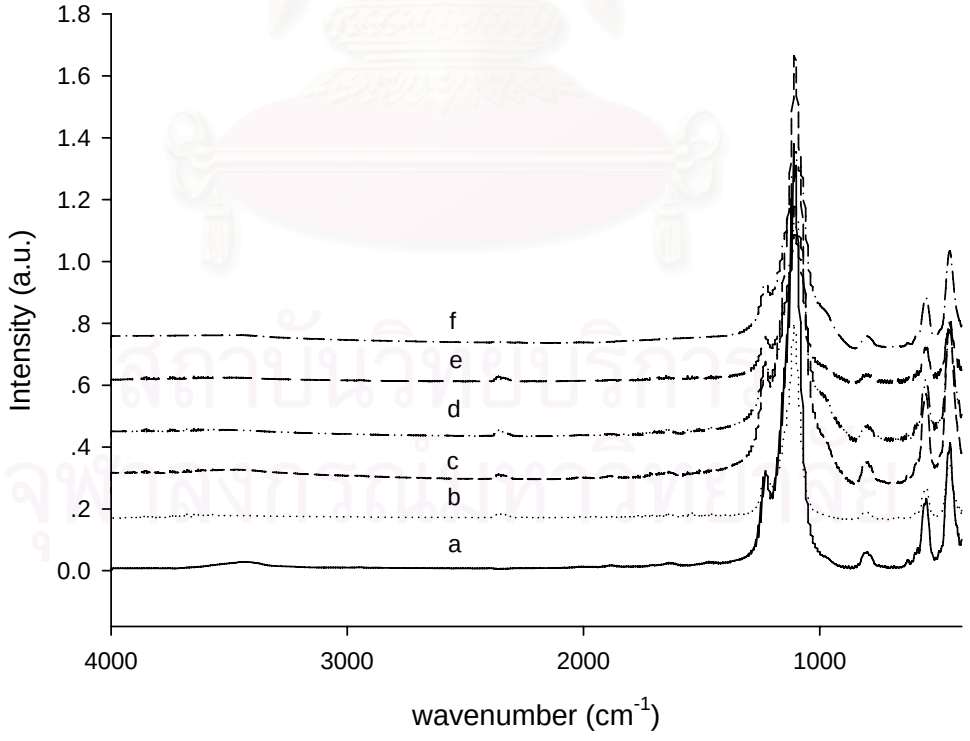

Figure 3 FT-IR spectra of TS-1 at various Si/Ti ratios of; a) 100, b) 50, c) 33, d) 25, e) 20, and f) 12

DR-UV spectra of the samples in Fig.4 show the strong peak at 210 nm, assigning to the tetracoordinated titanium in the zeolite framework. The broad band peak at 280 nm indicated the partially polymerized hexagonal coordinated Ti species, which contained Ti-O-Ti and belonged to a silicon-rich amorphous phase. The peaks at both 210 and 280 nm increased as titanium content increased. The peak at 280 nm increased stronger than that at 210 nm for the sample f due to the hexagonal coordinated Ti species formation at higher loaded[26]. XRD pattern shown in Fig. 5 was the calcined TS-1 samples containing an MFI phase with good crystallinity, no other diffraction peaks for contaminating crystalline and for non-zeolite phase were detected[27].

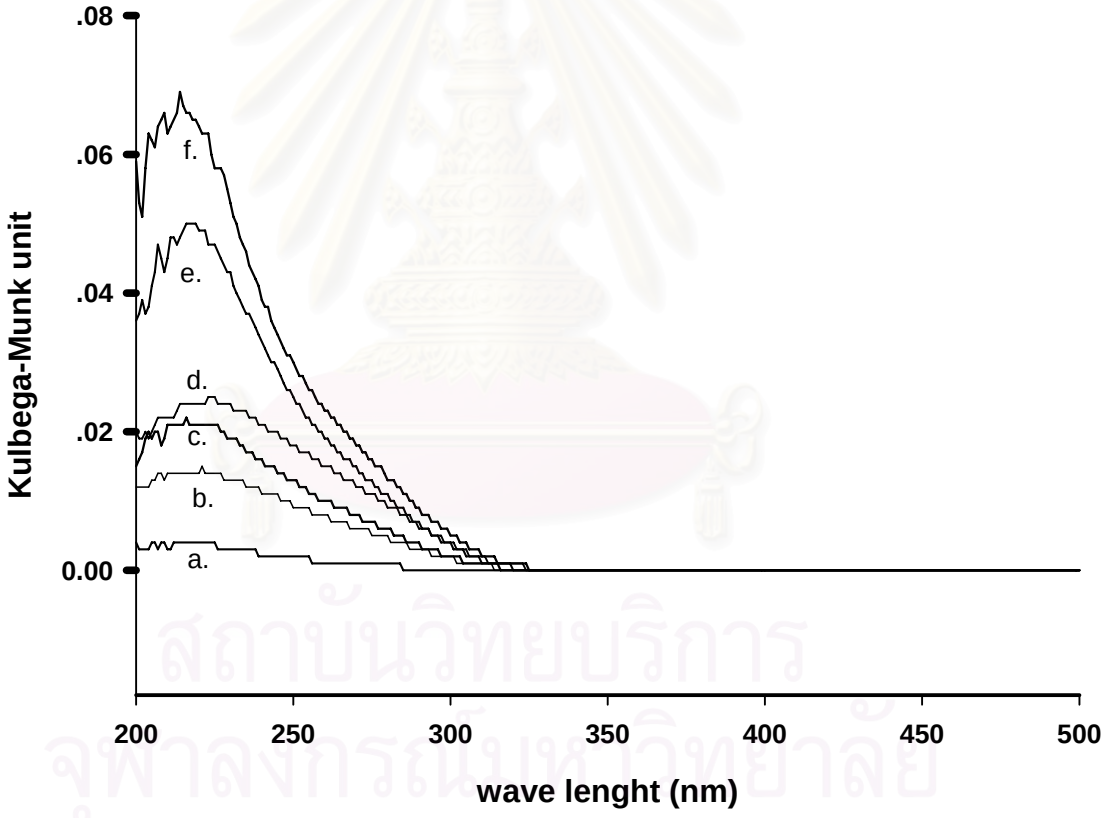

Figure 4 DR-UV spectra of TS-1synthesized at different ratios of; a) 100, b) 50, c) 33, d) 25, e) 20, and f) 12

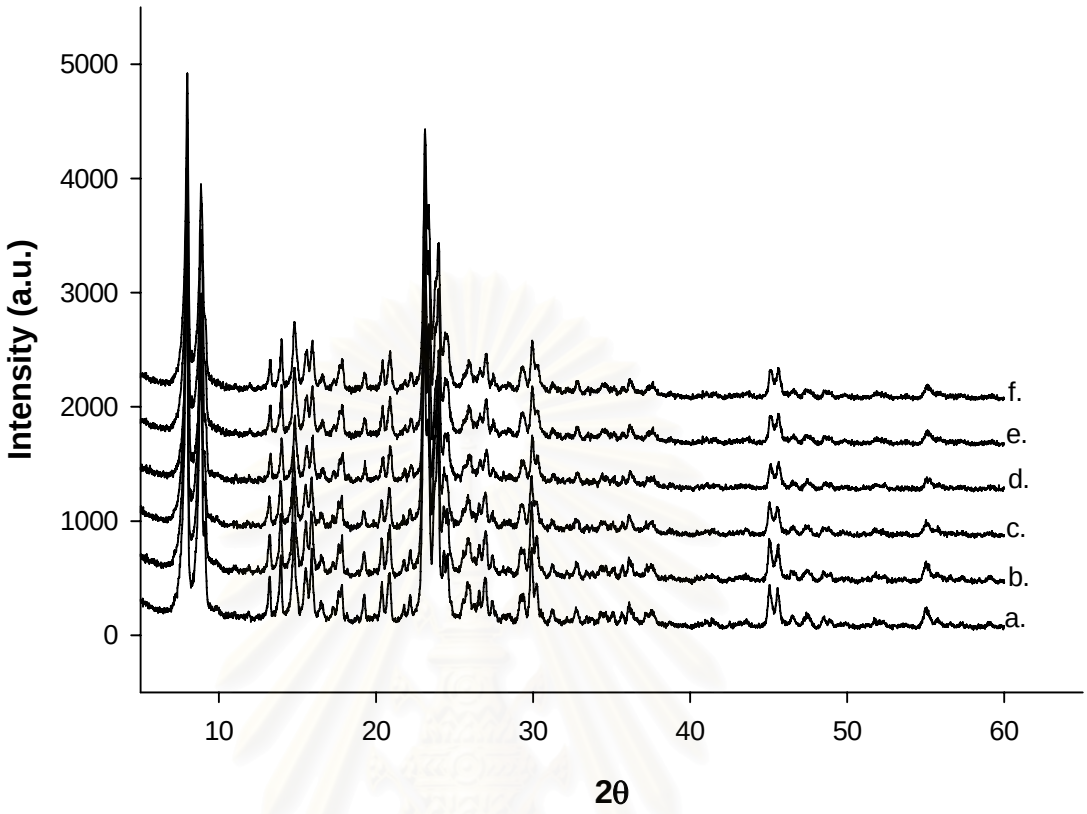

Figure 5 XRD patterns of calcined TS-1 at 550ºC for 2h with different Si/Ti ratios of; a) 100, b) 50, c) 33, d) 25, e) 20, and f) 12

The SEM micrographs and XRD patterns of TS-1 samples A-H are shown in fig. 6. All samples show the characteristics of TS-1 zeolite with the MFI structure.

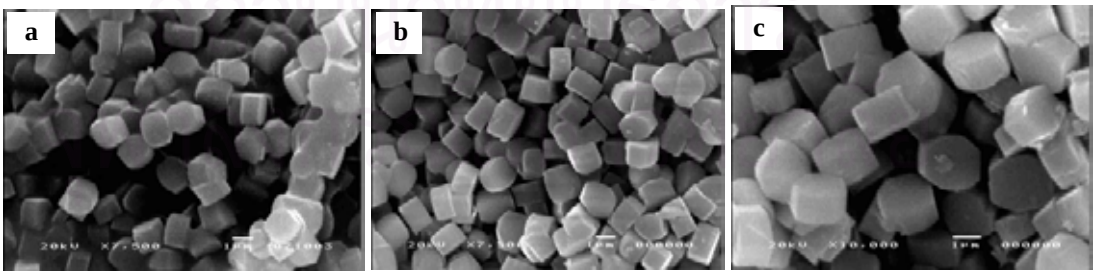

Figure 6 SEM micrographs of TS-1 samples at Si:Ti mole ratios of a) 100, b) 33, and c) 20

Surface area of TS-1 catalysts synthesized at different ratios of Si/Ti as shown in Table.2 gave no significant difference

Table 2 Surface area of TS-1 zeolite at different ratios of Si/Ti

Catalyst	Surface area (m^2/g)	Total Pore Volume (cc/g)
Si/Ti = 100	358	0.232
Si/Ti = 50	352	0.227
Si/Ti = 33	302	0.219
Si/Ti = 25	303	0.238
Si/Ti = 20	335	0.273
Si/Ti = 12	322	0.203

3. Bismuth titanate

FT-IR spectrum of the sample calcined at 600 ºC for 2 h is shown in Fig. 7. The peak was split into 4 peaks at 457, 525, 586 and 663 cm^{-1}, corresponding to the characteristic peaks of sillenite having Bi-O vibration modes, as reported by Carvalho et al.[28-29] The sharp peaks at 815 $cm^{-1}$and 937 cm^{-1} were not identified in the reference paper. Vasconcelos et al.[30] and Yao et al.[31] found similar phenomena and pointed out that the different data might be obtained from different samples. In Fig.8, the sharp peaks in the XRD pattern indicates a well crystallinity of prepared samples as those given in JCPDS data cards for $Bi_{12}TiO_{20}$. Figure 9 shows the DR-UV spectra in term of Kubelka-Munk function**.** It demonstrates information about the electronic transition and band gap of semiconductor. Akihito informed that it was a steep edge in a visible region due to an intrinsic band transition, not to the surface state[32].

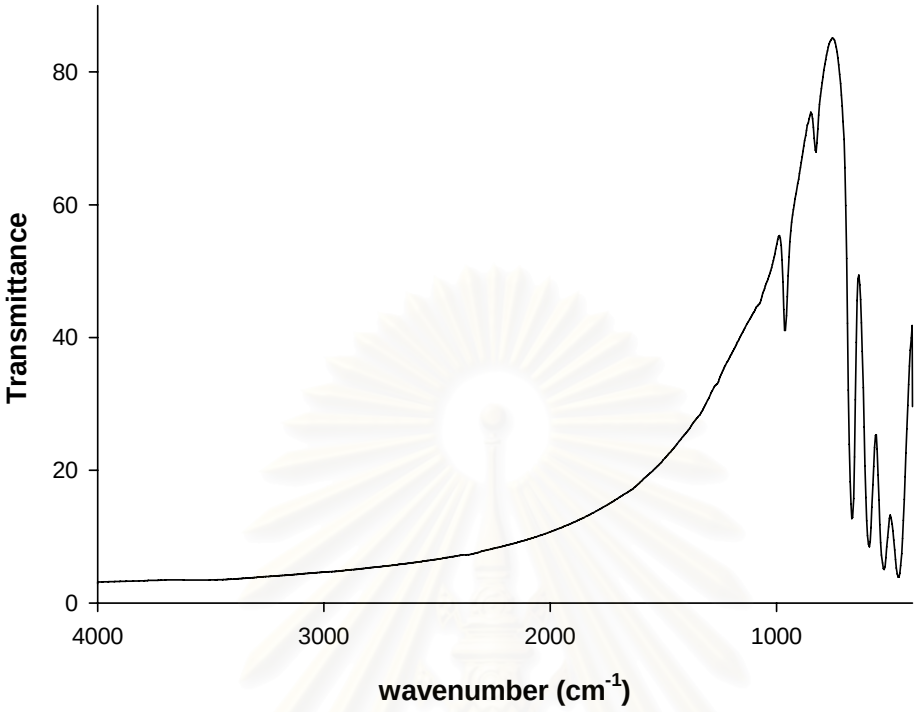

Figure 7 FT-IR spectrum of bismuth titanate after calcination at 600 ºC for 2 h

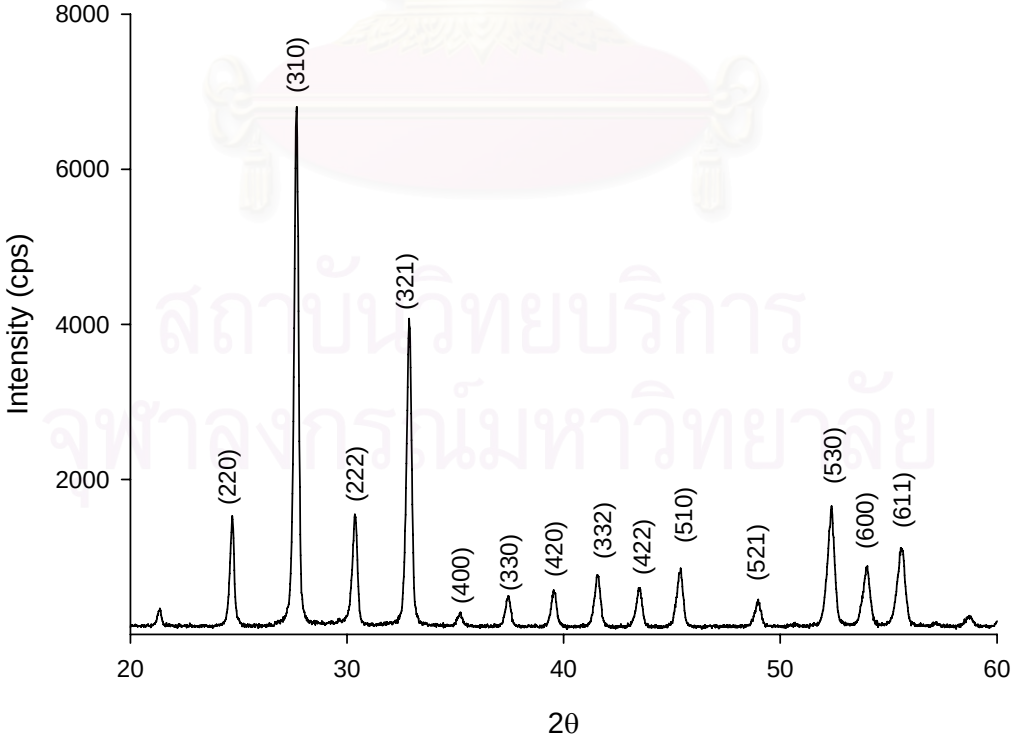

Figure 8 X-ray diffraction patterns of bismuth titanate powder after calcinations at 600 ºC in air for 2 h

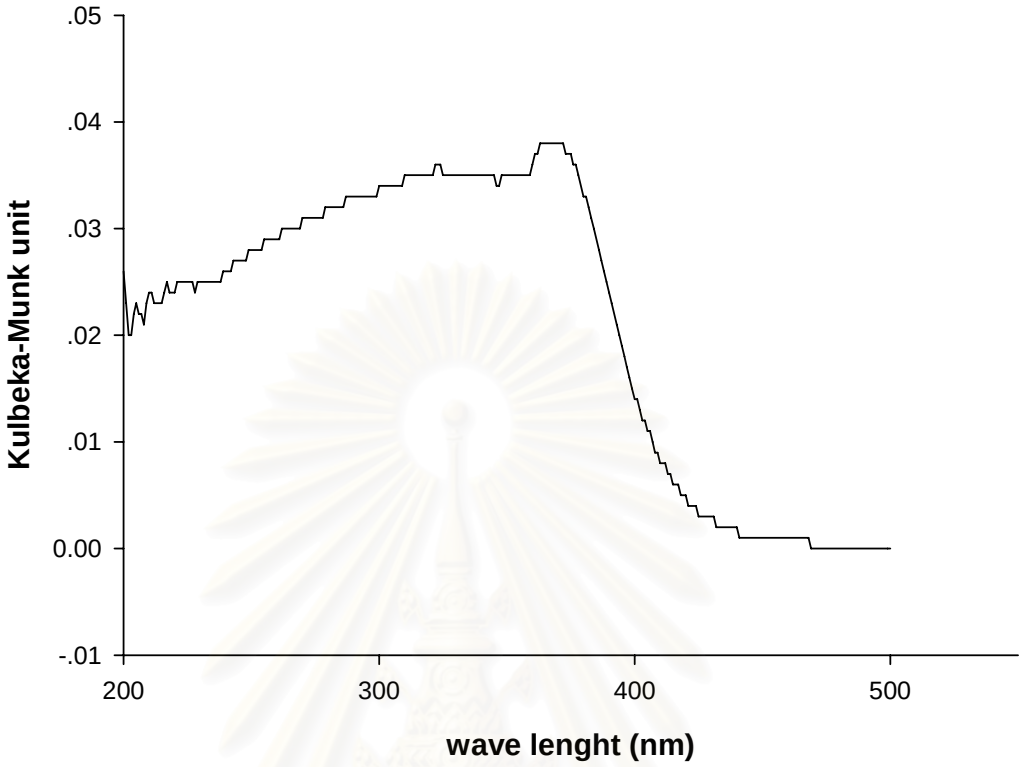

Figure 9 DR-UV spectrum of bismuth titanate calcined at 600 ºC for 2h

Photocatalytic Activity

1. pH variation effect

The experiments were carried out with a dye concentration of 40 ppm, at pH 3, 5, 7 and 9, for 6 h illumination time, using a 6 W UV-A lamp. The photocatalytic efficiency can be determined in term of decoloration (C/Co) and percent of mineralization $\mathrm{TOC} = 100 \times \left(\frac{\mathrm{TOC}_0 - \mathrm{TOC}}{\mathrm{TOC}_0} \right)$. The concentration of RB5 was measured using UV-Vis spectroscopy at 590 nm which is the maximum absorbance of the reactive black 5 dyes solution.

The photocatalytic activity of MCM-41 was shown in figure 10. From the results, the highest efficiencies of both the decoloration rate and the mineralization percentage were obtained at pH 3. The organic carbon was reduced to 22% of the initial carbon concentration.

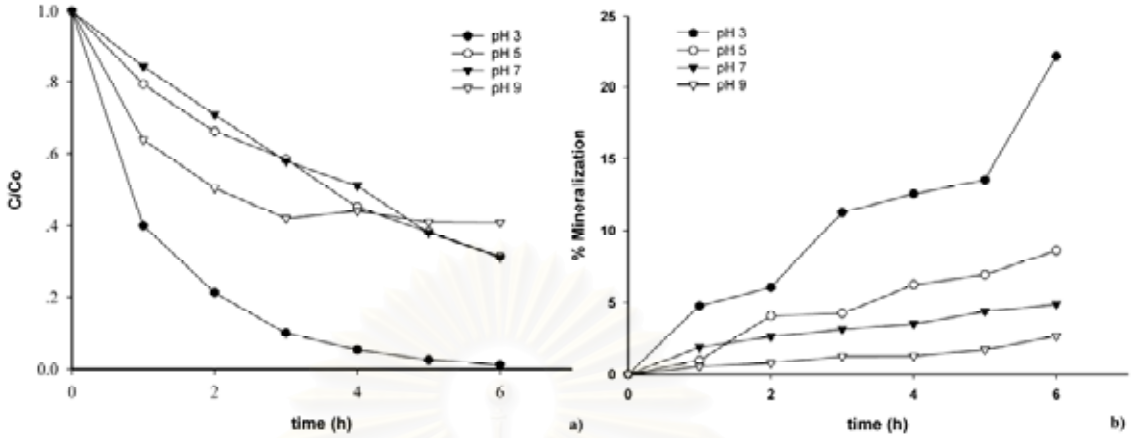

Figure 10 a) Decoloration and b) mineralization at various pHs (3, 5, 7 and 9) using MCM-41 zeolite catalyst

In the case of TS-1 zeolite catalyst, the activity of catalyst is quite different. The decoloration at various pHs was the same while the carbon reduction decreased, depending on the basic condition of the RB5 solution, see figure 11.

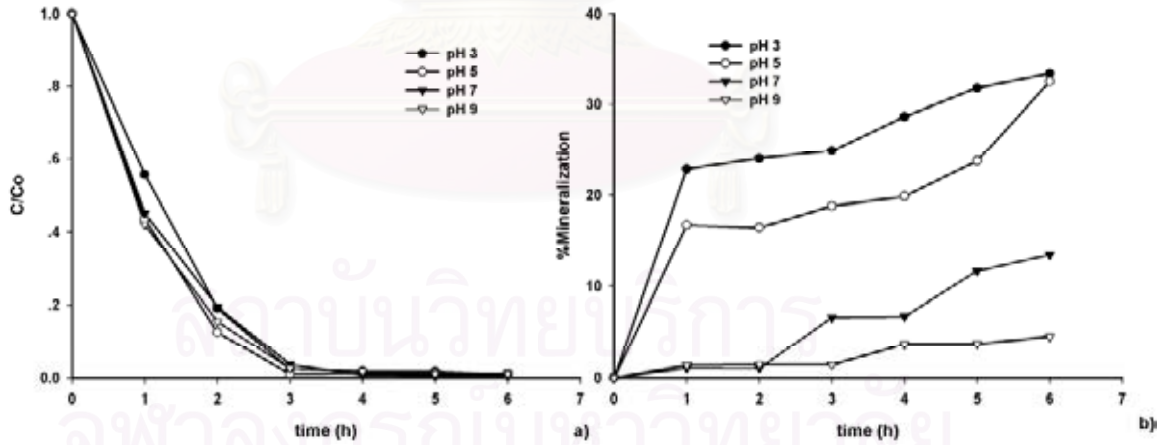

Figure 11 Effect of pH on a) decoloration and b) mineralization of RB5 using TS-1 catalyst with Si/Ti = 12 in the presence of 10 mM H_2O_2 at 25°C

Interestingly, variation in pH had no effect on both the decoloration and the mineralization of RB5 when using bismuth titanate catalyst, as seen in figure 12. However, it is clear that bismuth titanate does indeed show high photocatalytic

activity for the decoloration of RB5, consistent with previous studies by Matjaz and Danilo[17] of the decoloration of methyl orange. These results are presumably due to the presence of Bi-O polyhedra in the bismuth titanate crystal structure.

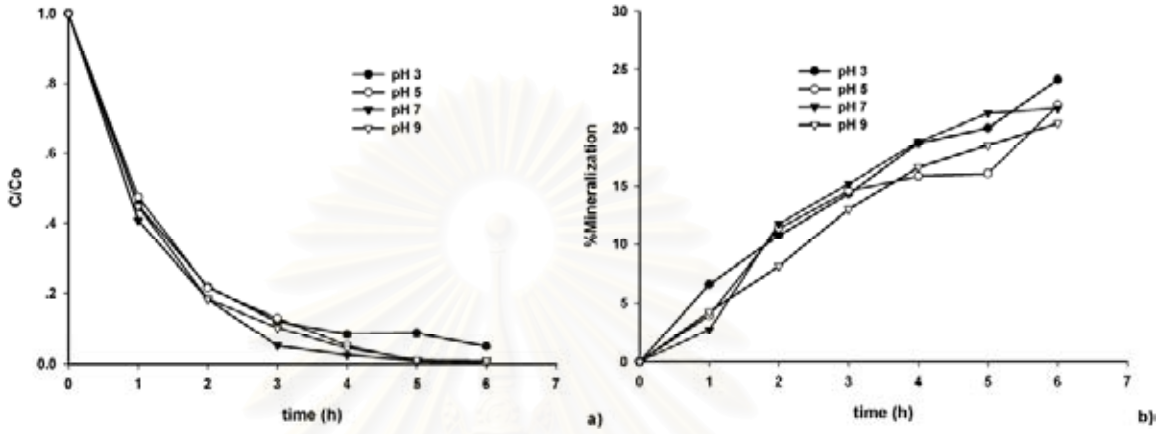

Figure 12 Effect of pH on a) decoloration and b) mineralization of RB5 using bismuth titanate catalyst in the presence of 10 mM H_2O_2 at 25°C

The degradation activities of three catalysts are different which pH parameter only affects to the decoloration of MCM-41 system while the organic carbon reduction in all system, using MCM-41; TS-1; bismuth titanate, occurred in the same trend.

This could be explained by considering adsorption and agglomeration phenomena. Haoqiang et al.[33] previously studied the effect of pH on photocatalytic degradation of acid azo dyes in aqueous TiO_2 suspensions, and found that the pH value changed the structure of the azo dye, as well as the surface charge density of the catalyst, and therefore affected the catalytic efficiency.

The structure of RB5 dye has a sulfonate group, which, when negatively charged, favors adsorption of the dye molecules on the positively charged surface of the catalyst. The zero point charge pH (pH_{zc}) for anatase TiO_2 is approximately 6.4. Since SiO_2 is more acidic than TiO_2, it is expected that the pH_{zc} of TS-1 may occur below pH 6.4.

For pH values lower than the pH_{iso} of TiO_2, the surface area of the catalyst becomes positively charged, and is negatively-charged at pH values higher than pH_{zc}. This observation suggests that electrostatic attraction will lead to dye adsorption at pH < 3.5[3], resulting in increased catalytic efficiency. On the other hand, electrostatic repulsions between charges on the catalyst surface and the dye molecules leads to dye agglomeration at pH > 6.4, resulting in a decrease of the efficiency. Thus, in highly acid media, RB5 dye molecules readily adsorb on the surface of the TS-1 zeolite catalyst, and, as a result, are effectively degraded with time.

An additional factor is that, in the presence of H_2O_2, TS-1 forms superoxo-Ti ($Ti(O_2^{\bullet -})$) and hydroperoxo-Ti (Ti(OOH)), reactive species that can generate hydroxyl radicals to react with dye molecules. It is reported that the peroxo complex formed in basic media has a higher stability than that formed in a neutral/acidic conditions[34-35]. Therefore, under basic conditions, hydroxyl radicals are generated less frequently than in acid conditions.

In the case of MCM-41, Li et al.[36] studied the advanced oxidation of orange II using TiO_2 supported on porous adsorbents and found that the pHzc of 50%TiO_2-MCM-41 equal to 6.9. Zhang et al[37] found that the charge-transfer excited state of the tetrahedrally coordinated titanium oxide species play important role in the direct photocatalytic decomposition of NO into N_2 and Wang et al[38] found Ti atom in this position exhibit high photocatalytic activity in the oxidation of C_2H_4. Thus, the reaction mechanism of MCM-41 will be passed through hydroxyl radical at Ti-tetrahedral in the framework.

Acidic solution the azo groups and the SO_3^- groups connected to the central naphtal are protonated. Thus, most hydroxyl radicals probably add to the azo groups although some also attacks the aromatic rings[39]. Moreover, the oxygen molecules in the air also influence on photocatalytic oxidation, as demonstrated in equations below[40]. Under acidic conditions, the steps for H_2O_2 production from oxygen are possible[41].

$$O_2 + e^- \longrightarrow O_2^{\bullet -} \quad (1)$$

$$O_2^{\bullet -} + H^+ \longrightarrow HO_2^{\bullet} \quad (2)$$

$$HO_2^{\bullet} + HO_2^{\bullet} \longrightarrow H_2O_2 + O_2 \quad (3)$$

While the photocatalytic reaction of MCM-41 and TS-1 passed through the generated hydroxyl radical in reactive species as Ti-center in the framework, bismuth titanate ($Bi_{12}TiO_{20}$) as semiconductor catalyst concerned electron-hole combination parameter. The photocatalytic mechanism of a semiconductor, such as TiO_2 or bismuth titanate, involves absorption of a photon in the band gap of the material, which generates electron hole-pairs in the semiconductor particles. Migration of the electron-hole pairs occurs to the surface of the catalyst, where trapping of electrons by adsorbed oxygen, or of holes by adsorbed hydroxyl ions, OH^-, results in the production of hydroxyl radicals, $^{\bullet}OH$, and oxidation of the adsorbed dye molecules[42-43]. Direct oxidation by reaction with holes (h^+) has also been reported[42]. The electron hole-pairs can recombine rapidly, so the interfacial electron transfer is kinetically competitive only when the relevant donor or acceptor is preadsorbed before photolysis[44]. In both acid and basic media, there is thus a small variation of degree of mineralization.

2. Amount of H_2O_2

RB5 can be degraded by hydroxyl radicals, $^{\bullet}OH$, as reactive species. Under UV-irradiation, H_2O_2 can be split photolytically to produce $^{\bullet}OH$ radical directly, which may enhance the reaction to some extent.

The reactivity of MCM-41 strongly depends on the amount of H_2O_2 as in figure 13. The decoloration rate and the percentage of organic carbon decomposition increased with higher dosage of oxidizing agent, H_2O_2, especially degree of carbon removal increasing from 20% to 60% mineralization.

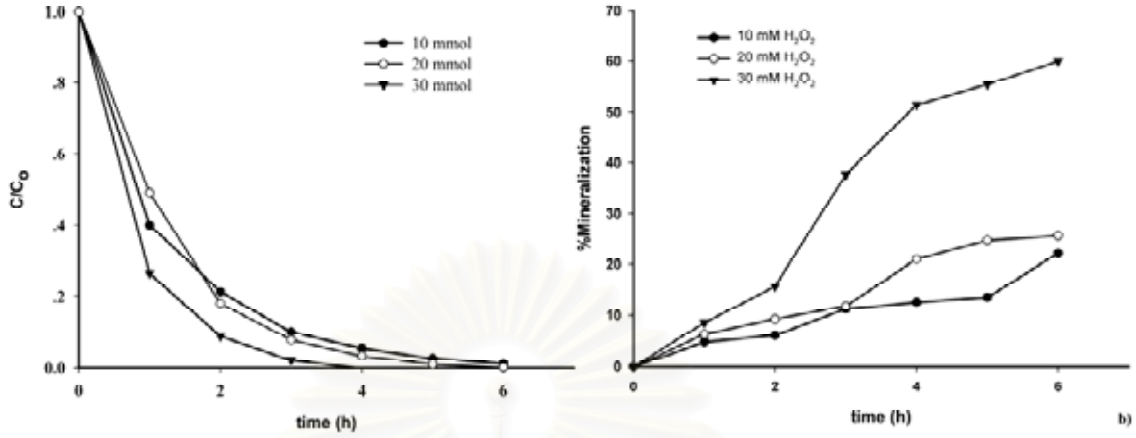

Figure 13 Influence of H_2O_2 concentration on a) decoloration and b) mineralization of RB5 using MCM-41 as catalyst at pH 3 and 25°C

In the presence of H_2O_2, titanium atoms in the TS-1 framework can form a reactive species, titanium-hydroperoxide complex, to react with the dye molecule. The O-O bond length in the titanium-hydroperoxide species, formed by the interaction of TS-1 with H_2O_2, is 1.52 Å[43] which represents a substantial activation of the O-O bond compared to that in H_2O_2 (1.49 Å)[9]. Decoloration efficiency and degree of mineralization therefore increases with a higher amount of H_2O_2. In this work, the highest dosage of H_2O_2 that generates the highest photocatalytic efficiency was determined to be 30 mM/l as in figure 14.

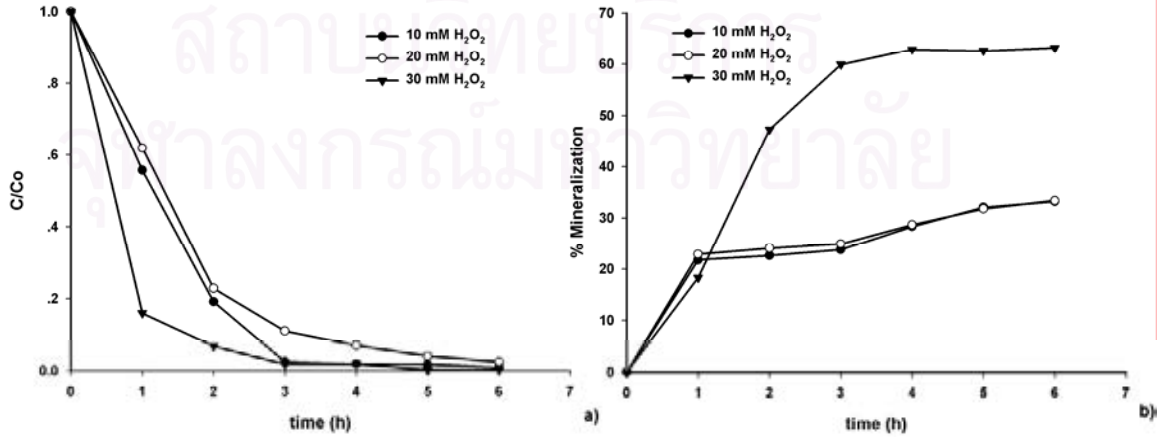

Figure 14 Influence of H_2O_2 concentration on a) decoloration and b) mineralization of RB5 using TS-1 as catalyst at pH 3 and 25°C

Due to the greater numbers of hydroxyl radicals generated from H_2O_2, the mineralization efficiency of the photocatalytic process is substantially enhanced. In the case of bismuth titanate, the effect of H_2O_2 level appears to be substantially smaller than that of TS-1, particularly with respect to the degree of mineralization as in figure 15. The enhanced reactivity in the presence of H_2O_2 is attributed in part to the fact that the resulting reactive radical intermediates exert a dual function: as strong oxidants themselves and as electron scavengers, thus inhibiting the electron-hole recombination at the semiconductor surface[44].

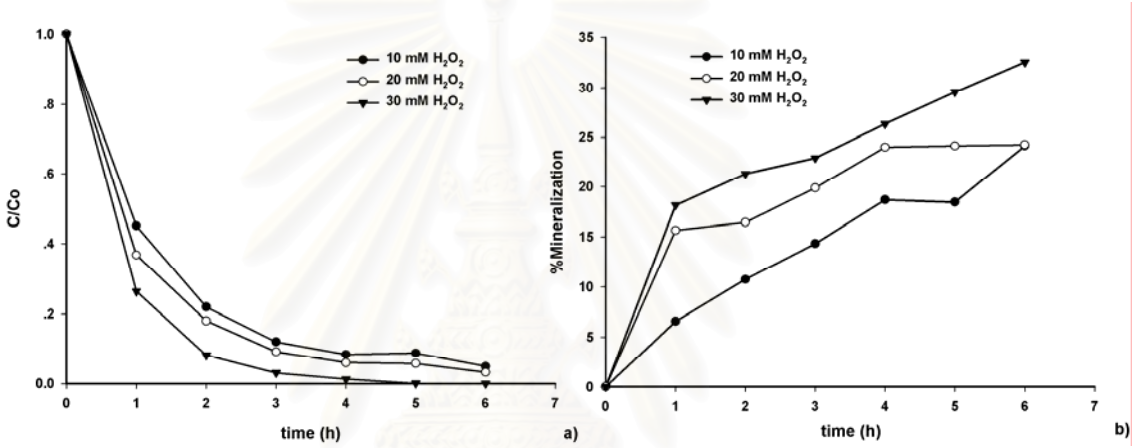

Figure 15 Influence of H_2O_2 concentration on a) decoloration and b) mineralization of RB5 using bismuth titanate as catalyst at pH 3 and 25°C

3. Ti content in MCM-41 and TS-1 synthesis

When photocatalytic degradation of reactive black 5 was performed at various amounts of Ti loaded MCM-41 (1, 2, 3, 4 and 5%) at pH 3 and 30 mmol H_2O_2, the results demonstrated that the more Ti -loaded onto MCM-41, the better degradation was observed, according to figure 16. Moreover, the performance of Ti-MCM-41 was better than that of TiO_2. The Ti-formed on MCM-41 supported catalyst indicated much fine particles than TiO_2 particle. In acidic solution a higher adsorption of dye on the catalyst leads to a faster decrease of the dye concentration. The results show that the degradation and decoloration of reactive black 5 are enhanced by the presence of Ti atom in the framework of MCM-41.

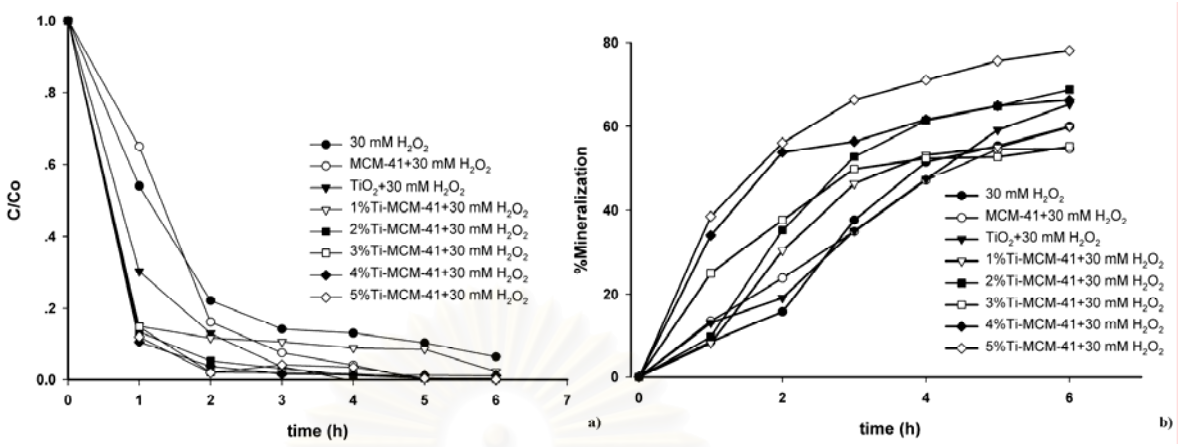

Figure 16 a) decoloration b) mineralization of photocatalytic oxidation process by various amounts of Ti loaded on MCM-41 (1, 2, 3, 4 and 5%), without catalyst, TiO_2 , and MCM-41.

As figure 17, the decoloration performance does not vary significantly with Si/Ti ratio. In contrast, the degree of mineralization increases significantly as the Si/Ti ratio decreases, and exhibits a remarkable enhancement for an Si/Ti ratio of 12.

In the TS-1 structure, Brønsted acid sites, which react with peroxide to form catalytically-active titanium peroxide, arise from formation of tetrahedral Si-O-Ti species[45]. As decreasing the Si/Ti ratio from 100 to 12, the number of Brønsted acid sites increase. The fact that decoloration occurs faster than mineralization suggests that the $^{\bullet}OH$ radicals react first at the azo bond, which is the chromophore of the RB5 dye.

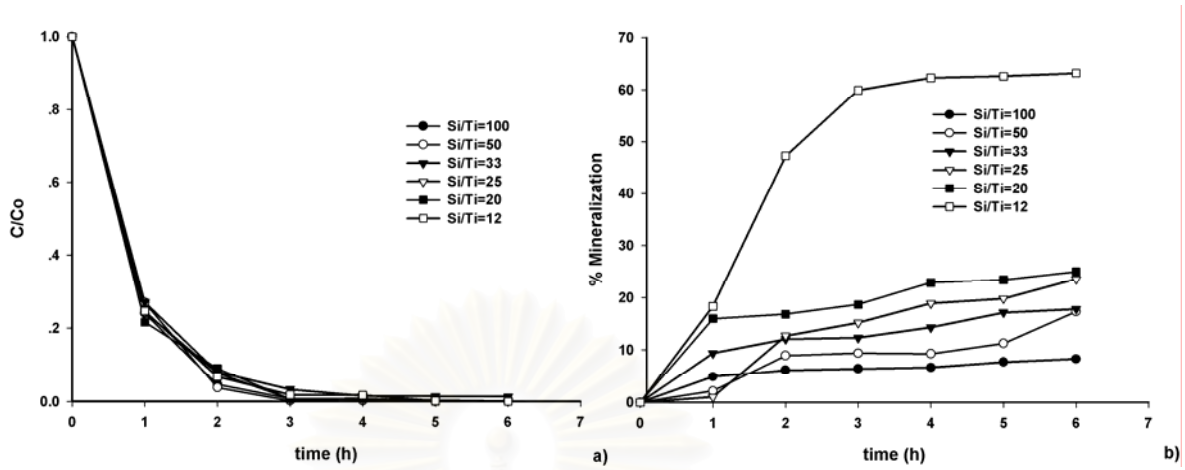

Figure 17 a) Decoloration and b) mineralization of RB5 in the presence of 30 mM H_2O_2 at pH 3 and 25°C using various Si/Ti ratios of TS-1 zeolite catalysts

4 .Kinetic analysis

The Langmuir-Hinshelwood (L-H) model was used to determine the photodegradation kinetics of the dye. The second order of dye decomposition can be expressed as

$$r = k' C_O C_{OH} \quad (1)$$

where r is the initial degradation rate, k' is the surface second order rate constant, C_O and C_{OH} are the initial concentrations of the dye and the ·OH radical, respectively. If the concentration of very active ·OH radicals takes on a steady-state value of the process, the decoloration kinetics can be simplified to a pseudo-first-order rate expression. The second-order rate equation can be rewritten as follows:

$$-\frac{d[C]}{dt} = k_{app} Co \quad (2)$$

where Co represents initial concentration of the dye and C is the concentration of the dye at time t. The pseudo-first-order kinetic constant was calculated from the slope of plot of ln(Co/C) versus time at each condition.

The reaction rate and half life of each condition are summarized in Table 3. Due to the highest surface area and the large pore size, MCM-41 exhibits the highest reaction rate which around ten times of using TS-1 and bismuth titanate.

Table 3 Reaction rates of the photocatalytic process using Ti-MCM-41, TS-1, bismuth titanate (BTO)

Catalyst	Condition	Reaction Rate ($x10^{-3}$ min^{-1})	Half Life (min)
MCM-41	1%Ti-MCM-41	88.27	47.12
	2%Ti-MCM-41	124.48	33.41
	3%Ti-MCM-41	126.85	32.784
	4%Ti-MCM-41	128.03	32.64
	5%Ti-MCM-41	135.67	30.65
Si:Ti	Si:Ti = 100	14.59	59.77
	Si:Ti = 50	14.77	46.91
	Si:Ti = 33	14.05	68.95
	Si:Ti = 25	13.96	49.64
	Si:Ti = 20	13.50	49.48
BTO	BTO	13.24	52.35

5. Photocatalytic activity of MCM-41, TS-1 and bismust titanate in waste water

Because waste water from industry has lots of chemical components which could be not identified in real situation, the screening test with the parameters of pH and amount of H_2O_2 was carried out.

5.1 pH parameter

As shown in figure 18, the maximum decoloration rate was obtained at pH 3 since MCM-41 decomposed the organic pollutant only in acidic media. For organic carbon removal, around 10% mineralization was obtained at pH 3.

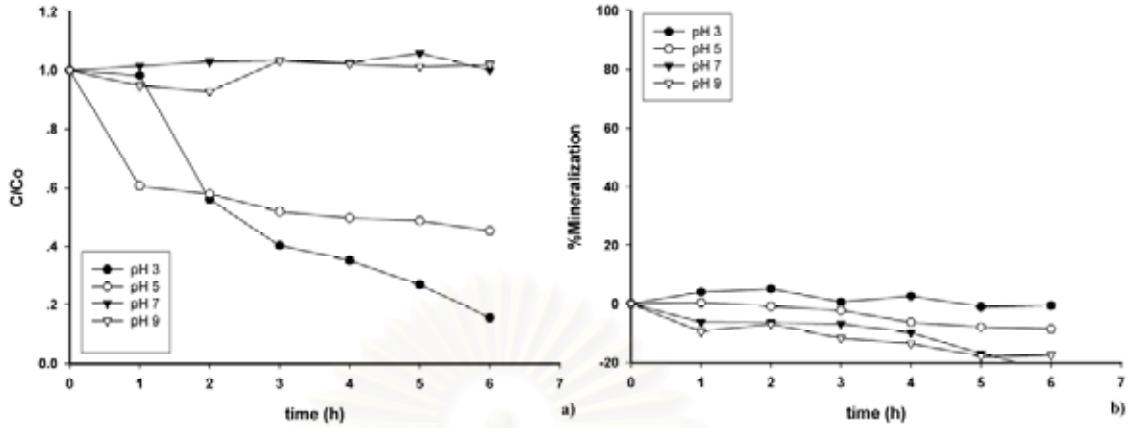

Figure 18 a) decoloration and b) mineralization of waste water at various pHs using 1%Ti-MCM-41

Figure 19 shows the reactivity of TS-1. The catalyst reduced the color of waste water in some extent at neutral media. The degree of mineralization was achieved around 10%, similar to the result of MCM-41.

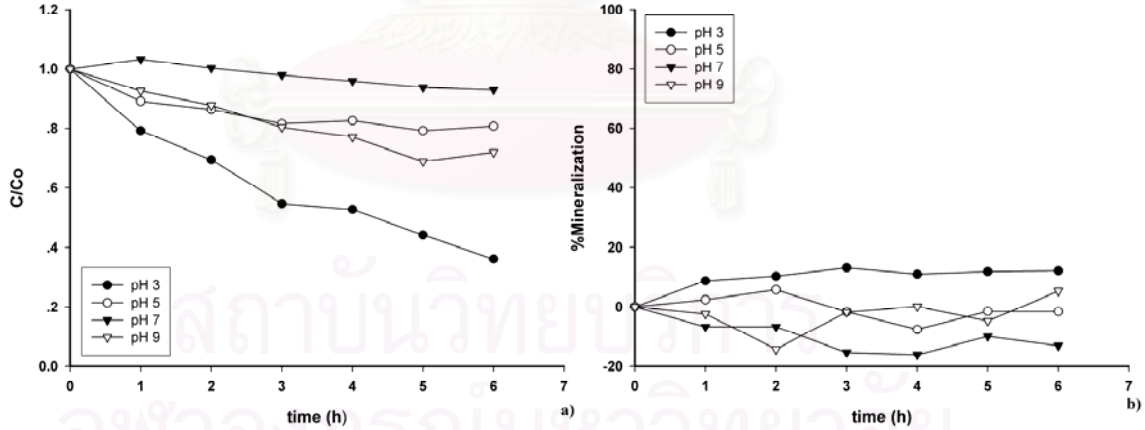

Figure 19 a) decoloration and b) mineralization of waste water at various pHs using 1%Ti-TS-1 (Si/Ti=100)

Bismuth titanate catalyst activity is also similar to the activity of the MCM-41. It could decolorize organic pollutant only in acid media, but the oxidation power to oxidize some organic pollutant to CO_2 was quite low, see figure 20.

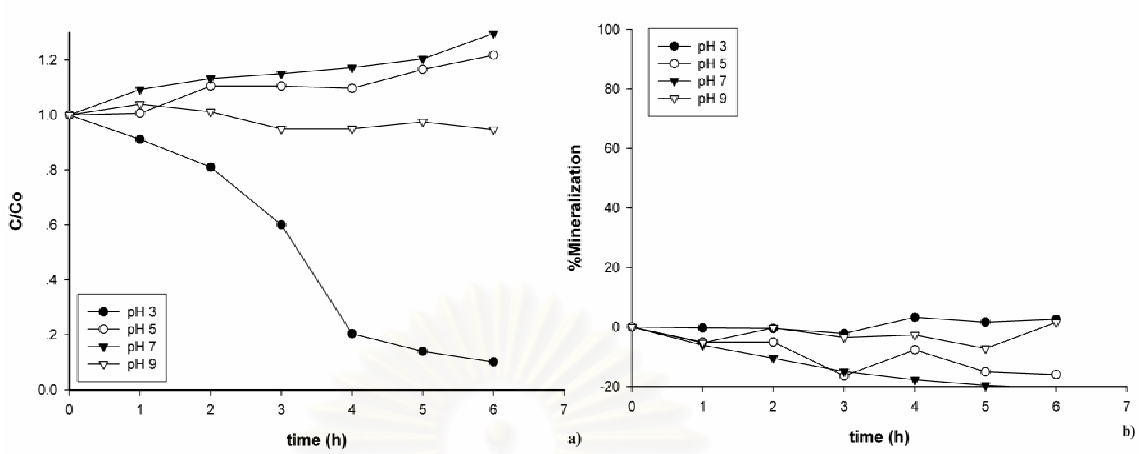

Figure 20 a) decoloration and b) mineralization of waste water at various pHs using bismuth titanate as catalyst

5.2 Amount of H_2O_2

From figures 21-23, when the amount of H_2O_2 increased the decoloration and the degree of mineralization increased in all system. MCM-41 still exhibits the highest activity among the three catalysts. The decoloration characteristics of both MCM-41 and TS-1 at 60 mM of H_2O_2 give the same trend. It can be suggested that this phenomena occurred from Ti-tetrahedral coordination in zeolite framework utilizing hydroxyl radicals to attack dye molecules, as studied for the RB5 system.

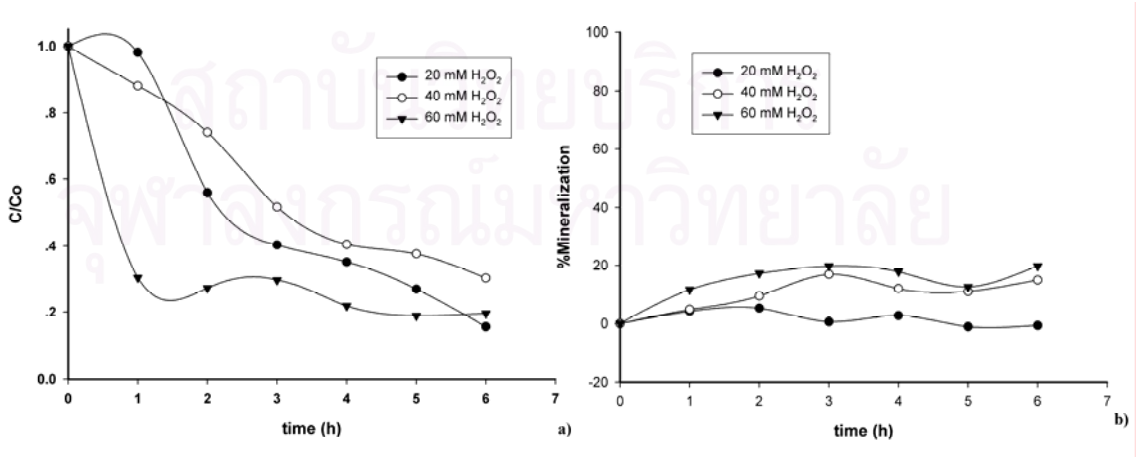

Figure 21 a) decoloration and b) mineralization of waste water using 1%Ti-MCM-41 at various H_2O_2 concentrations.

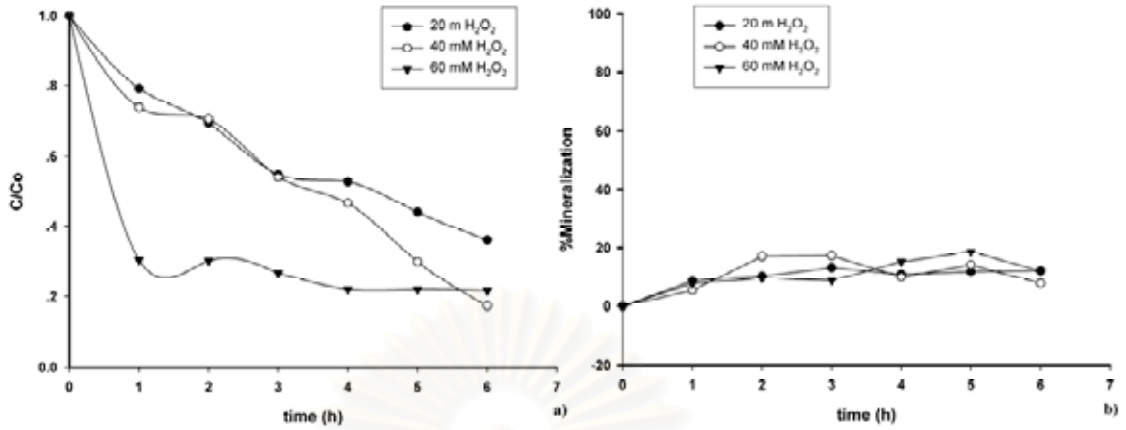

Figure 22 a) decoloration and b) mineralization of waste water using 1%Ti-TS-1 (Si/Ti=100) at various H_2O_2 concentrations.

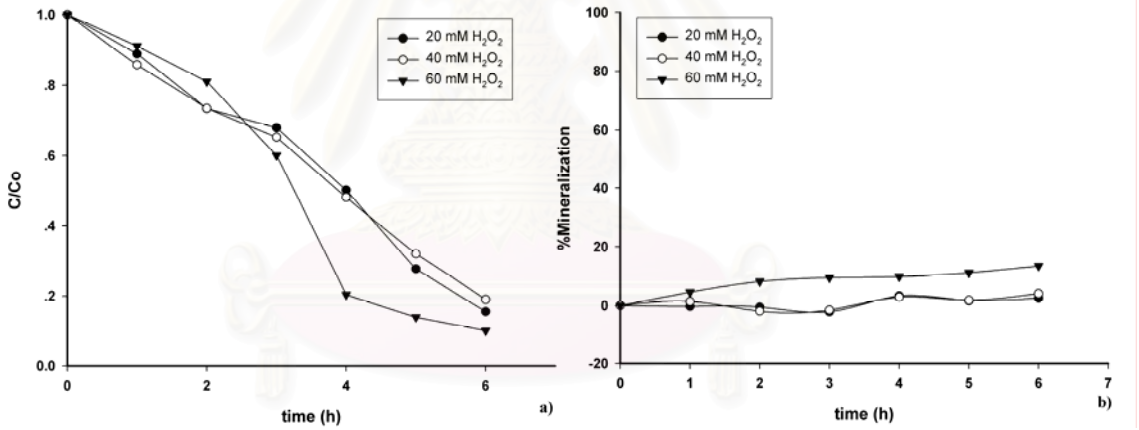

Figure 23 a) decoloration and b) mineralization of waste water using bismuth titanate at various H_2O_2 concentrations.

From the screening test results, the optimal condition from the RB5 system was applied to the waste water system. Again, MCM-41 shows the highest decoloration, see Figure 23, followed by TS-1, TiO_2, and $Bi_{12}TiO_{20}$ (bismuth titanate) respectively. Interestingly, in the absence of catalyst, H_2O_2 itself could not decolorize the waste water, unlike the RB5 system. It is worth noting that the conditions used in this study is very mild, 6W-UV light, 0.5g/l of catalyst and 60 mM H_2O_2, and this

might be the reason why the organic carbon removal was low (19% maximum using 5%Ti-MCM-41).

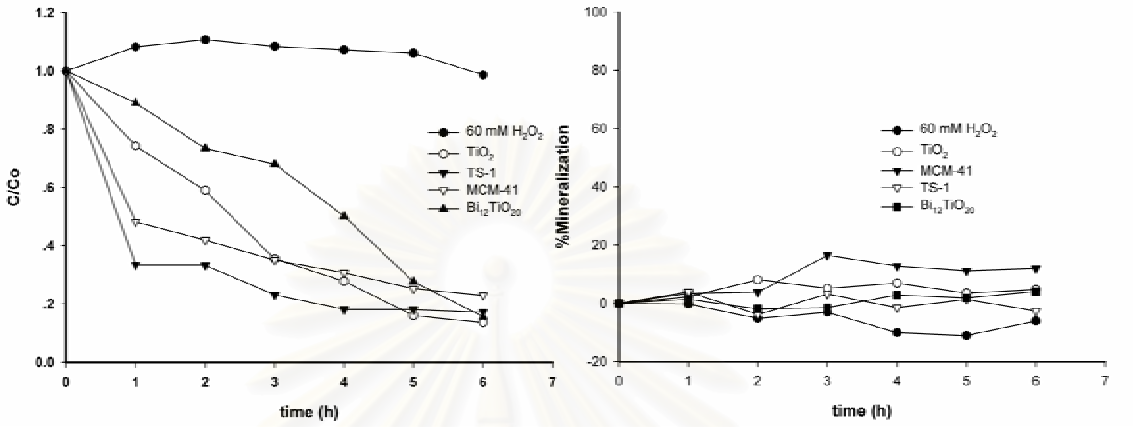

Figure 24 a) decoloration and b) mineralization of waste water using the optimal condition from the investigation of RB5 system, 5%Ti-MCM-41, Si/Ti = 12 ratio of TS-1 and bismuth titanate at pH3, 60 mM H_2O_2

Conclusions

The photocatalytic performance of MCM-41, TS-1, and bismuth titanate for the oxidation of RB5 was evaluated under a 6 W UV-A lamp. The highest photocatalytic activity was achieved at pH3 in the presence of H_2O_2 for all systems. The decoloration rate was not significantly different when comparing TS-1 versus bismuth titanate. Higher dosage of H_2O_2 increased the decoloration rate of reaction. The degree of mineralization achieved by MCM-41 and TS-1 (with high Ti loading, Si/Ti = 12) was twice higher than bismuth titanate due to the uniform distribution of reactive Ti-centers in the zeolite framework, enhancing the reaction process.

For the case of the waste water obtained from industry, MCM-41 demonstrated the highest efficiency both in decoloration and mineralization (19% organic carbon removal), orderly followed by TS-1, TiO_2, bismuth titanate, and 60 mM H_2O_2-without catalyst.

References

1. U. Pagga, D. Brown, Chemosphere 15 (1986) 479–491.
2. M.A. Brown, S.C. De Vito, Crit. Rev. Environ. Sci. Technol. 23 (1993) 249.
3. E. Kusvuran, O. Gulnaz, S. Irmak, O.M. Atanur, H.I. Yavuz, O. Erbatur, J. Hazard. Mater. B109 (2004) 85–93.
4. K. Tanaka, K. Padermpole, T. Hisanaga, Water Res. 34 (2000) 327–333.
5. I. Arslan, I.A. Balcioglu, D.W. Bahnemann, Dyes Pigments 47 (2000) 207–218.
6. I.K. Konstantinou, T.A. Albanis, Appl. Catal. B: Environ. 49 (2004) 1–14.
7. A. Aguedach, S. Brosilon, J. Morvan, E.K. Lhadi, Appl. Catal. B: Environ. 57 (2005) 55-62.
8. M.R. Hoffmann, S.T. Martin, W. Choi, D.W. Bahnemann, Chem. Rev. 93 (1993) 341.
9. T. Torimoto, Y. Okawa, N. Takeda, H. Yoneyama, J. Photochem. Photobiol. A: Chem. 103 (1997), 1501.
10. S.S. Hong, C.S. Ju, C.G. Lim, B.H. Ahn, K.T. Lim, G.D. Lee, J. Ind. Eng. Chem. 7 (2) (2001) 99.
11. H. Yamashita, Y. Ichihashi, M. Anpo, M. Hashimoto, C. Louis, M. Che, J. Phys. Chem. 100 (1996) 16041.
12. M. Anpo, H. Yamashita, Y. Ichihashi, Y. Fuji, M. Honda, J. Phys. Chem. B 101 (1997) 2632.
13. W.S. Ahn, D.H. Lee, T.J. Kim, J.H. Kim, G. Seo, R. Ryoo, Applied Catalysis A: General, 181, (1999) 39-49.
14. A. Bhaumik, T. Tatsumi, Journal of Catalysis, 189, (2000) 31–39.
15. R.J. Davis Z. Liu. Chemistry of Materials, 9, (1997) 2311-2324.
16. W.F. Yao, H. Wang, X.X. Hong, X.F. Cheng, J. Huang, S.X. Shang, X.N. Yang, M.Wang, App. Catal. A: Gen. 243 (2003) 185–190.
17. V. Matjaz, S. Danilo, J. Am. Ceram. Soc. 84 (2001) 2900-2904.
18. N. Thanabodeekij, W. Tanglumlert, E. Gulari, S. Wongkasemjit, Applied Organomethallic Chemistry, 19 (2005) 1047-1054.
19. N. Phonthammachai, M. Krissanasaeranee, E. Gulari, A.M. Jamieson, S. Wongkasemjit. Mat. Chem. and Phys. 97 (2006) 458-467.

20. N. Thanabodeekij, E. Gulari, S. Wongkasemjit. Powder Technology 160 (2005) 203 – 208.
21. P. Piboonchaisit, S. Wongkasemjit, R. Laine, Science-Asia, J. Sci. Soc.Thailand 25 (1999) 113–119.
22. N. Phonthammachai, T. Chairassameewong, E. Gulari, A.M. Jamieson, S. Wongkasemjit, J. Met. Mater. Min. 12 (2002) 23.
23. M.Chatterjee, H. Hayashi, N. Saito. Microporous and Mesoporous Materials, 57 (2003) 143–155.
24. L. Marchese, T. Maschmeyer, E. Gianotti, S. Coluccia, and J.M. Thomas. J. Phys. Chem. B, 101 (1997) 8836-8838.
25. D. Scarano, A. Zecchina, S. Bordiga, J. Chem. Soc. Faraday Trans. 89 (1993) 4123.
26. A. Thangaraj, R. Kumar, S.P. Mirajkar, P. Ratnasamy, J. Catal. 130 (1991) 1.
27. X.S. Wang, X.W. Guo, G. Li, Catalysis Today. 74 (2002) 65-75.
28. J.F. Carvalho, R.W.A. Franco, C.J. Magon, L.A.O. Nunes, F. Pellegrini, A.C. Hernandes, Mater. Res. 2 (2) (1999) 87.
29. J.F. Carvalho, R.W.A. Franco, C.J. Magon, L.A.O. Nunes, F. Pellegrini, A.C. Hernandes, Opt. Mater. 13 (1999) 333.
30. I.F. Vasconcelos, M.A. Pimenta, A.S. B. Sombra, J. Mater. Sci. 36 (3) (2001) 587.
31. W.F. Yao, H. Wang, X.X. Hong, D. Wang, X.N.Yang, M.Wang, S.X. Shang, J. Mat. Sci. Lett. 21 (2002) 1803-1805.
32. K. Akihito, I. Mikami, Chem. Lett. 10 (1998) 1027.
33. Z. Haoqiang, C. Kongchang, T. He, Dyes and Pigments 37(1998) 241-247.
34. G. Tozzola, M.A. Mantegazza, G. Ranghino, G. Petrini, S. Bordiag, G. Ricchiardi, C. Lamberti, R. Zulian, A. Zecchina, J. Catal. 179 (1998) 64-71.
35. V.N. Shetti, D. Srinivas, P. Ratnasamy, J. Molec. Catal. A: Chem. 210 (2004) 171-178.
36. G. Li, X.S. Zhao, Madhumita B. Ray, Separation and Purification Technology 55 (2007) 91–97.
37. J. Zhang, M. Minagaw, T. Ayusaw, S. Natarajan, H. Yamashit, M. Matsuok, M. Anpo, J. Phys. Chem. B 104 (2000) 11501.

38. X. Wang, W. Lian, X. Fu, J.M. Basset, Frédéric Lefebvre, J. Catalysis 238 (2006) 13–20.
39. K. Dajka, E. Takacs, D. Solpan, L. Wojnarovits, O. Guven, Radiation Physics and Chemistry. 67 (2003) 535-538.
40. C. Tang and V. Chen, Water research, 38 (2004) 2775-2781.
41. A. Houas, H. Lachheb, M. Ksibi, E. Elaloui, C. Guillard, J.M. Herrmann, App. Catal. B: Envi. , 31(2) (2001) 145-157.
42. P. Reeves, R. Ohlhausen, D. Sloan, K. Pamplin, T. Scoggins, C. Clark, B. Hutchinson, D.Green, Solar Energy 48 (6) (1992) 413-420.
43. S. Naskar, S.A Pillay, M. Chanda, J. Photochem and Photobiol A: Chem. 113 (3) (1998) 257-264.
44. E. Karlsen, K. Schöffel, Catal. Today. 32 (1996) 107-114.
45. C.K. Gratzel, M. Jirousek, M. Gratzel, J. Mol. Catal. 60 (1990) 375-387.

สถาบันวิทยบริการ
จุฬาลงกรณ์มหาวิทยาลัย

Appendix

R. Wisedsri, A.M. Jamieson and S. Wongkasemjit, Comparison of TS-1 zeolite to bismuth titanate photocatalysts for waste water treatment using reactive black 5 dye as model, to be published in the book entitled “Advanced Metals and Metal Oxides Technology”.

สถาบันวิทยบริการ
จุฬาลงกรณ์มหาวิทยาลัย

Comparison of TS-1 zeolite to bismuth titanate photocatalysts for waste water treatment using reactive black 5 dye as model

R. Wisedsri, A.M. Jamieson, and S. Wongkasemjit

Abstract

The photocatalytic degradation of reactive black 5, a non-biodegradable dye, in the presence of hydrogen peroxide, was investigated by comparing two custom-made catalysts, viz. TS-1 zeolite and $Bi_{12}TiO_{20}$. The effect of pH, H_2O_2 concentration and Si/Ti ratio of the zeolite was explored, as assessed by degree of decoloration and mineralization (loss of total organic content). Experiments were conducted under low power of 6 W UV-A irradiation. We found that, whereas the decoloration rate of each catalyst was comparable and insensitive to pH, the degree of mineralization achieved by TS-1 diminished strongly with pH while that achieved by $B_{12}TiO_{20}$ was insensitive to pH change. This reflects that oxidative attack first occurs at the azo bond of the dye molecule, which is the source of color. Lower Si/Ti ratio (higher Ti loading) of TS-1 exhibits good catalytic efficiency up to 65% mineralization of RB5. The activation energies of TS-1 and bismuth titanate catalyst are 18.71 and 25.35 kJ/mol, respectively. The mineralization percentage achieved by TS-1 (Si/Ti = 12) was twice as high as that of $B_{12}TiO_{20}$ although the decoloration rate was not significantly different. The high catalytic efficiency indicates that the TS-1 zeolites tested have exceptionally high levels of catalytically active framework Ti which is uniformly distributed throughout the zeolite pore volume.

Introduction

Azo dyes constitute the largest and most important class of commercial dyes in wastewater. They are mostly non-biodegradable and resistant to destruction by conventional wastewater treatments [1]. The discharge of highly colored wastewater into the ecosystem generates environmental problems such as aesthetic pollution (even a small amount of dye is highly visible), and perturbation of aquatic life [2].

Recent studies indicate that toxic and refractory organic compounds including dyes in wastewater can be destroyed by advanced oxidation processes (AOPs) [3-5]. Photocatalytic degradation (UV/TiO_2) is one AOP which is receiving increased attention, because of the low cost and relatively high chemical stability of the catalyst, and the possibility to use sunlight as the source of irradiation [6]. Moreover, photocatalysis does not require expensive oxidants and can be carried out under mild temperature and pressure [7]. TiO_2 is known to be the most active photocatalyst for organic oxidation [8]. However, there are certain limitations in using bare TiO_2 in photocatalytic reactors. For example, due to their small size (about 4-30 nm), TiO_2 particles aggregate rapidly in a suspension, losing effective surface area, as well as catalytic efficiency. Being non-porous, TiO_2 exhibits a low ability to absorb pollutants [9]. Therefore, inserting titanium within the cavities which exist in the framework of zeolites, as, for example, in titanium silicalite (TS-1), may be advantageous, because zeolites have nanoscale pores, and high adsorption capacities and ion-exchange capacities [10-12].

Another interesting catalyst is bismuth titanate ($Bi_{12}TiO_{20}$), which is reported to have high photocatalytic activity for decoloration of methyl orange [13]. Some part of this material has the absorption onset wavelength of visible region (around 500 nm), meaning that it has a possibility to use under weak UV light or may be sunlight. The $Bi_{12}TiO_{20}$ crystal belongs to a family of compounds known as sillenites, which have the general formula $Bi_{12}MO_{20}$, where M represents a tetravalent cation, or a combination of ions with an average charge of 4+. The framework of the $Bi_{12}TiO_{20}$ crystal structure is formed by Bi–O polyhedra, in which Bi ions are coordinated to five oxygen ions in an octahedral arrangement together with the stereochemically active $6s^2$ electron lone pair of Bi^{3+}. The Bi-O polyhedron network connects to geometrically regular TiO_4 tetrahedra. Each tetrahedron is formed by four oxygen anions with the Ti cation occupying the tetrahedral interstice [14].

Catalyst activity of TS-1 and $Bi_{12}TiO_{20}$

Both catalysts were synthesized according to references 15-16. Photocatalytic activity of both TS-1 and bismuth titanate was evaluated not only with respect to the effects of pH and H_2O_2 concentration, but also with regard to the Ti level in TS-1, to

assess whether these parameters had any influence on both coloration, represented as the ratio of the dye concentration at time t to the initial dye concentration, $\frac{C}{C_0}$, and mineralization, calculated as percent reduction in $TOC = 100 \times \left(\frac{TOC_0 - TOC}{TOC_0} \right)$ where TOC_0 and TOC are total organic contents at time 0 and t, respectively.

Effect of pH

The experiments were carried out with a dye concentration of 40 ppm, at pH 3, 5, 7 and 9, for 6 h illumination time, using a 6 W UV-A lamp. The effect of pH on decoloration and mineralization efficiency of RB5, using TS-1 with an Si/Ti ratio of 12, is illustrated in Figure 1. The results indicate that, increase of pH does not significantly reduce the efficiency of decoloration of RB5, but the degree of mineralization is substantially altered. The mineralization dramatically decreases when the pH increases to 7 and 9. Adsorption and agglomerization of dye molecules are two key factors which influence the photocatalytic degradation of RB5 [20]. These factors strongly depend on the pH of the solution.

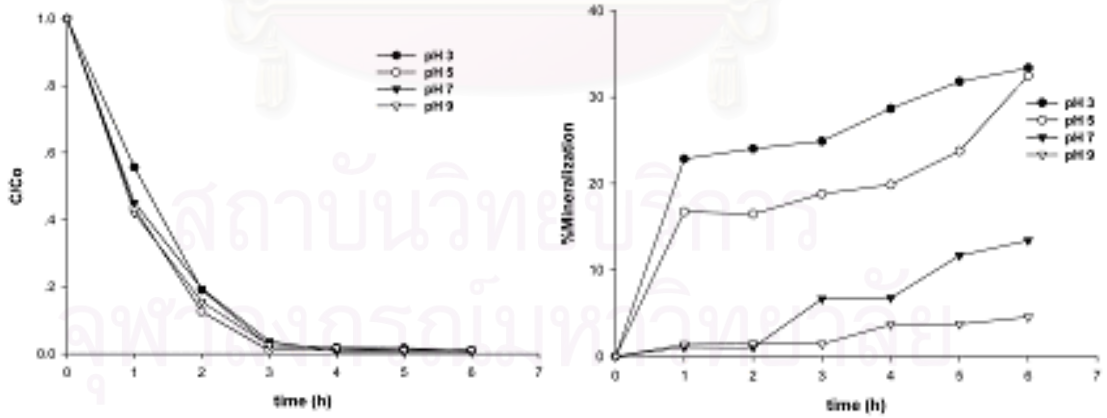

a) **b)**

Figure 1 Effect of pH on a) decoloration and b) mineralization of RB5 using TS-1 catalyst with Si/Ti = 12 in the presence of 10 mM H_2O_2 at 25°C

Zhan et al. [21] have previously studied the effect of pH on photocatalytic degradation of acid azo dyes in aqueous TiO_2 suspensions, and found that the pH value changes the structure of the azo dye, as well as the surface charge density of the catalyst, and therefore affects the catalytic efficiency. The structure of RB5 dye has a sulfonate group, which when negatively charged, favors adsorption of the dye molecules on the positively charged surface of the catalyst. The isoelectric pH (pH_{iso}) is 3.5 and the zero point charge pH (pH_{zc}) for anatase TiO_2 is approximately 6.4. Since SiO_2 is more acidic than TiO_2, it is expected that the pH_{zc} of TS-1 may occur below pH 6.4. For pH values lower than the pH_{iso} of TiO_2, the surface area of the catalyst becomes positively charged, and is negatively-charged at pH values higher than pH_{zc}. This observation suggests that electrostatic attraction will lead to dye adsorption at pH < 3.5 [3], resulting in increased catalytic efficiency. On the other hand, electrostatic repulsions between charges on the catalyst surface and the dye molecules leads to dye agglomeration at pH > 6.4, resulting in a decrease of the efficiency. Thus, in highly acid media, RB5 dye molecules readily adsorb on the surface of the TS-1 zeolite catalyst, and, as a result, are effectively degraded with time.

An additional factor is that, in the presence of H_2O_2, TS-1 forms superoxo-Ti ($Ti(O_2^{\bullet -})$) and hydroperoxo-Ti (Ti(OOH)), reactive species that can generate hydroxyl radicals to react with dye molecules. It is reported that the peroxo complex formed in basic media has a higher stability than that formed in a neutral/acidic conditions [22-23]. Therefore, under basic conditions, hydroxyl radicals are generated less frequently than in acid conditions.

Interestingly, variation in pH had no effect on both the decoloration and the mineralization of RB5 when using bismuth titanate catalyst, as seen in Figure 2. However, it is clear that bismuth titanate does indeed show high photocatalytic activity for the decoloration of RB5, consistent with previous studies by Matjaz and Danilo [13] of the decoloration of methyl orange. These results are presumably due to the presence of Bi-O polyhedra in the bismuth titanate crystal structure.

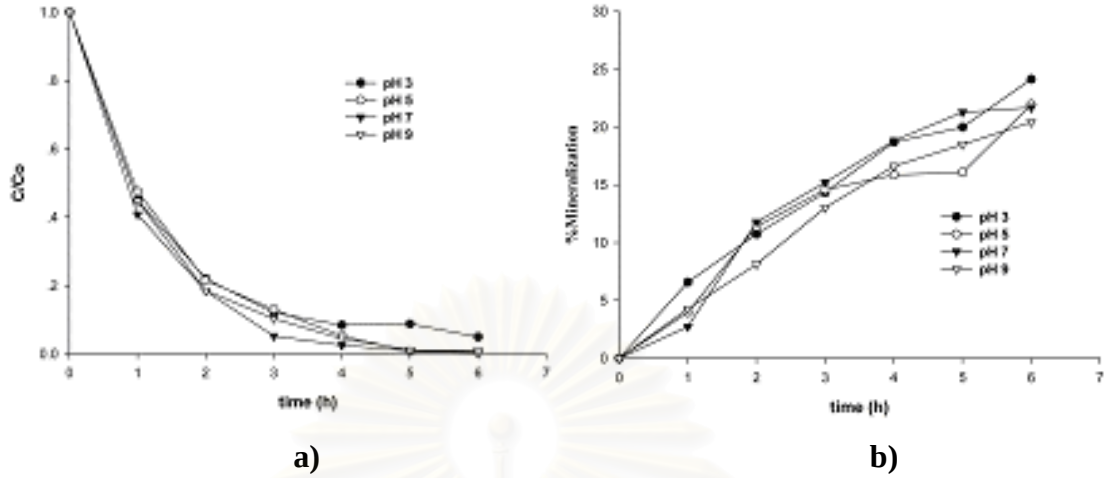

a) **b)**

Figure 2 Effect of pH on a) decoloration and b) mineralization of RB5 using bismuth titanate catalyst in the presence of 10 mM H_2O_2 at 25°C

The photocatalytic mechanism of a semiconductor, such as TiO_2 or bismuth titanate, involves absorption of a photon in the band gap of the material, which generates electron hole-pairs in the semiconductor particles. Migration of the electron-hole pairs occurs to the surface of the catalyst, where trapping of electrons by adsorbed oxygen, or of holes by adsorbed hydroxyl ions, OH^-, results in the production of hydroxyl radicals, $^{\bullet}OH$, and oxidation of the adsorbed dye molecules [24-26]. Direct oxidation by reaction with holes (h^+) has also been reported [24]. The electron hole-pairs can recombine rapidly, so the interfacial electron transfer is kinetically competitive only when the relevant donor or acceptor is preadsorbed before photolysis [27]. In both acid and basic media, there is thus a small variation of degree of mineralization.

Effect of peroxide addition

It has been reported that RB5 can be degraded by hydroxyl radicals, $^{\bullet}OH$, as reactive species [20]. Under UV-irradiation, H_2O_2 can be split photolytically to produce $^{\bullet}OH$ radical directly, which may enhance the reaction to some extent. In the presence of H_2O_2, titanium atoms in the TS-1 framework can form a reactive species, titanium-hydroperoxide complex, to react with the dye molecule. The O-O bond length in the titanium-hydroperoxide species, formed by the interaction of TS-1 with

H_2O_2, is 1.52 Å [28] which represents a substantial activation of the O-O bond compared to that in H_2O_2 (1.49 Å) [10]. Decoloration efficiency and degree of mineralization therefore increases with a higher amount of H_2O_2. In this work, the highest dosage of H_2O_2 that generates the highest photocatalytic efficiency was determined to be 30 mM/l (Figures 3 and 4). Due to the greater numbers of hydroxyl radicals generated from H_2O_2, the mineralization efficiency of the photocatalytic process is substantially enhanced as seen in Figures 3b and 4b. In the case of bismuth titanate, the effect of H_2O_2 level appears to be substantially smaller than for TS-1, particularly with respect to the degree of mineralization. The enhanced reactivity in the presence of H_2O_2 is attributed in part to the fact that the resulting reactive radical intermediates exert a dual function: as strong oxidants themselves and as electron scavengers, thus inhibiting the electron-hole recombination at the semiconductor surface [29].

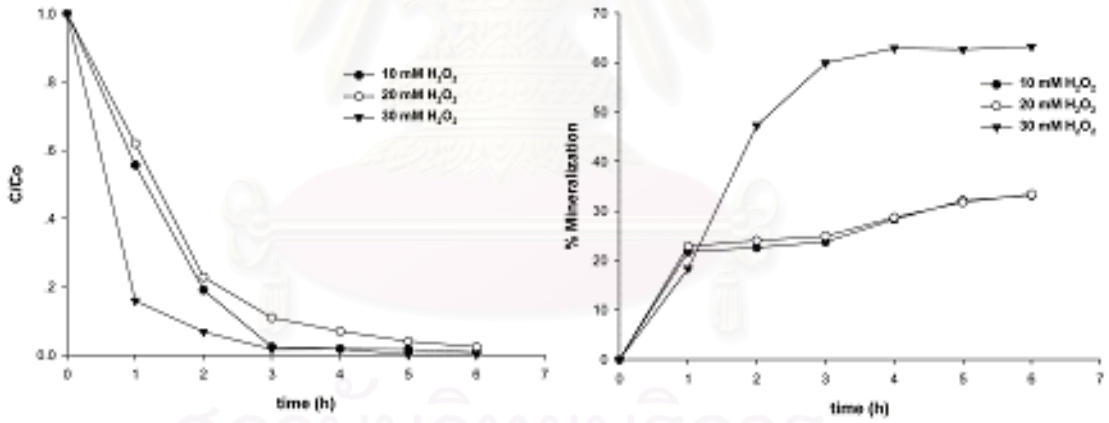

a) **b)**

Figure 3 Effect of H_2O_2 concentration on a) decoloration and b) mineralization of RB5 using TS-1 zeolite catalyst with Si/Ti = 12 at pH 3 and 25°C

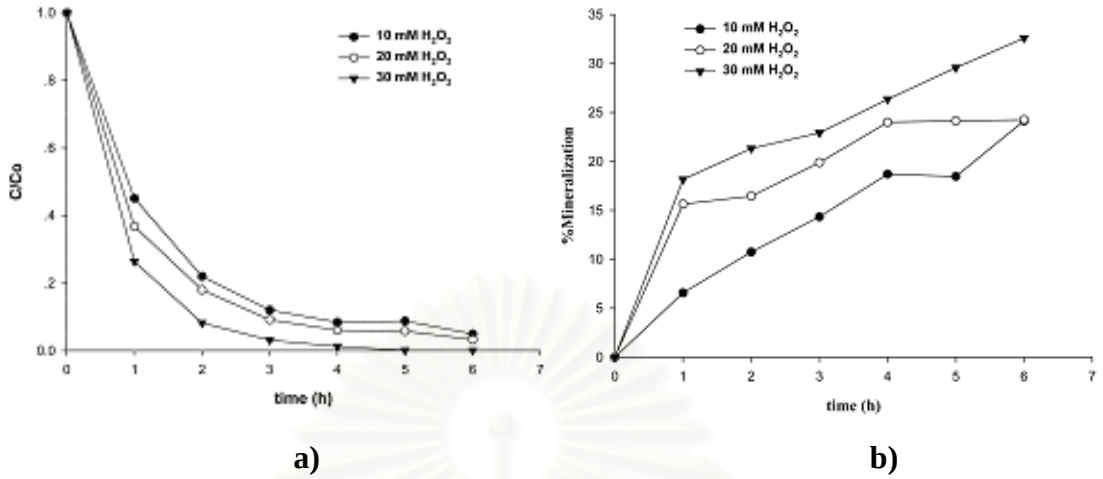

a) **b)**

Figure 4 Influence of H_2O_2 concentration on a) decoloration and b) mineralization of RB5 using bismuth titanate as catalyst at pH 3 and 25°C

Effect of Si/Ti ratio

Lower Si/Ti ratio means higher titanium content in the zeolite framework. The Si/Ti ratios in a mixture solution containing silatrane and titanium glycolate precursors and in TS-1 final product investigated using inductively coupled plasma (ICP) spectrometer are shown in Table 1. It is shown that most of titanium species added into the reaction of TS-1 formation were reacted. Figure 5a shows the decoloration of RB5 using TS-1 with various Si/Ti ratios. The decoloration performance does not vary significantly with Si/Ti ratio. In contrast, the degree of mineralization increases significantly as the Si/Ti ratio decreases, and exhibits a remarkable enhancement for an Si/Ti ratio of 12.

Table 1 Si/Ti ratios in the starting precursor mixture and TS-1 final product using ICP spectroscopy

Si:Ti ratio (starting materials)	Si:Ti ratio (final product)
100	98.6
50	50.1
33	33.4
25	26.9
20	20.3
12	10.4

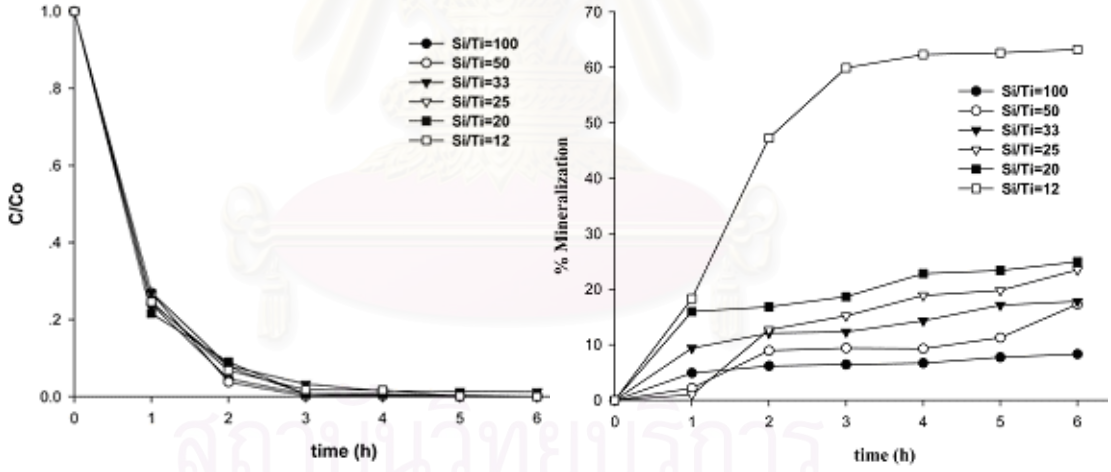

a) **b)**

Figure 5 a) Decoloration and b) mineralization of RB5 in the presence of 30 mM H_2O_2 at pH 3 and 25°C using various Si/Ti ratios of TS-1 zeolite catalysts

In the TS-1 structure, Brønsted acid sites, which react with peroxide to form catalytically-active titanium peroxide, arise from formation of tetrahedral Si-O-Ti species [30]. As decreasing the Si/Ti ratio from 100 to 12, the number of Brønsted

acid sites increase. The fact that decoloration occurs faster than mineralization suggests that the $^{\bullet}OH$ radicals react first at the azo bond, which is the chromophore of the RB5 dye.

Kinetic Analysis

1. Reaction rate and adsorption coefficient

The Langmuir-Hinshelwood (L-H) model was used to determine the photodegradation kinetics of the dye. The second order of dye decomposition can be expressed as

$$r = k' C_O C_{OH} \quad (1)$$

where r is the initial degradation rate, k' is the surface second order rate constant, C_O and C_{OH} are the initial concentrations of the dye and the $^{\bullet}OH$ radical, respectively. If the concentration of very active $^{\bullet}OH$ radicals takes on a steady-state value of the process, the decoloration kinetics can be simplified to a pseudo-first-order rate expression. The second-order rate equation can be rewritten as follows:

$$-\frac{d[C]}{dt} = k_{app} Co \quad (2)$$

where Co represents initial concentration of the dye and C is the concentration of the dye at time t. The pseudo-first-order kinetic constant was calculated from the slope of plot of ln(Co/C) versus time at each condition.

The reaction rate and half life of each condition are shown in Table 2. From the results, pH, dosage of H_2O_2 and Si/Ti ratio effects do not rapidly change the reaction rate. When the amount of H_2O_2 increases from 10 mM/l to 30 mM/l, the reaction rate of TS-1 goes up from 11.52 x 10^{-3} to 13.17 x 10^{-3} min^{-1} and bismuth titanate from 9.06 x 10^{-3} to 13.24x 10^{-3} min^{-1}. The smaller increase of reaction rate can suggest that the dosage of H_2O_2 has reached a maximum efficiency to decolorize the RB5. This study conforms to Lucas et al. [31] who investigated the H_2O_2 effect for RB5 dye with Fenton's reagent-yeast. They found that if the dosage of H_2O_2 reached a certain value, the decoloration efficiency did not significantly improve.

Table 2 Reaction rates of the photocatalytic process using TS-1, bismuth titanate (BTO), bismuth oxide, titanium dioxide, silicon dioxide and no catalyst

Catalyst	Condition	Reaction Rate ($x10^{-3}$ min^{-1})	Half Life (min)
TS-1 (Si:Ti=12)	pH 3[a]	11.52	60.17
	pH 5	11.38	60.91
	pH 7	10.50	65.99
	pH 9	10.81	64.11
	10 mM[b]	11.52	60.17
	20 mM	12.13	57.60
	30 mM	13.17	52.60
Si:Ti	Si:Ti = 100[b]	14.59	59.77
	Si:Ti = 50	14.77	46.91
	Si:Ti = 33	14.05	68.95
	Si:Ti = 25	13.96	49.64
	Si:Ti = 20	13.50	49.48
BTO	pH 3[a]	9.06	76.49
	pH 5	11.18	61.99
	pH 7	10.68	64.89
	pH 9	10.40	66.63
	10 mM[b]	9.06	76.49
	20 mM	10.27	58.50
	30 mM	13.24	52.35
Bismuth Oxide	30 mM[b]	13.30	52.10
Titanium dioxide	30 mM[b]	7.89	87.90
Silicon dioxide	30 mM[b]	16.54	41.89
H_2O_2 no catalyst	30 mM[b]	18.85	36.77

[a] using 10 mM of H_2O_2

[b] at pH 3

สถาบันวิทยบริการ
จุฬาลงกรณ์มหาวิทยาลัย

From Table 2 the reaction rate was affected by the turbidity resulted from catalyst particles blocking UV-absorption of H_2O_2 molecule, causing H_2O_2 not to be able to become reactive radicals to react with dye or other organic molecule. Moreover, high turbidity solution reduced light penetrability to dyes; consequently, the direct oxidation of dye with electron transfer from TiO_2 particles was reduced. This result responded to Tang et al. [32] who also studied the photocatalytic degradation of reactive black 5 using TiO_2/UV in an annular photoreactor. High turbidity solution from TiO_2 leaded to reduction of efficiencies of catalyst. In the absence of catalyst, the kinetic reaction rate was highest followed by SiO_2. The TiO_2 as catalyst had the lowest reaction rate because it has a large turbidity while the reaction rate of Bi_2O_3 was close to bismuth titanate and TS-1. Although bismuth oxide does not have Bi-O polyhedra in crystal structure like bismuth titanate, the presence of this bond may help reduce the recombination of electron-hole in bismuth oxide semiconductor particle, as discussed previously, Bi-O polyhedra in crystal structure could help reduce the recombination of electron-hole recombination [13].

2. Activation energy

The activation energy of the reaction can be assumed to generally follow the Arrhenius law:

$$k_{app} = k_o \exp\left[-\frac{E_a}{RT}\right], \qquad (3)$$

where E_a is apparent activation energy, R is the gas constant, k_o is a constant pre-exponential factor, and k_{app} is a pseudo-first-order rate constant of decoloration. The reaction rates were studied at various temperatures ranging from 15°-35°C, as shown in Table 3.

The linear transformation of Eq. 3 is

$$\ln k_{app} = \ln k_o - \frac{E_a}{RT} \quad . \qquad (4)$$

The activation energy was obtained from the plot of $\ln k_{app}$ versus $\frac{1}{T}$. The slope is equal to $-\frac{E_a}{R}$. Figure 6 shows the correlations between $\ln k_{app}$ and $\frac{1}{T}$ of TS-1 and bismuth titanate, as followed Eq. 5 for TS-1 and Eq. 6 for bismuth titanate:

$$\ln k_{app} = 3.17 - \frac{2.25}{T} \qquad R^2 = 0.97 \qquad (5)$$

$$\ln k_{app} = 5.89 - \frac{3.07}{T} \qquad R^2 = 0.93. \qquad (6)$$

The activation energies of the reaction calculated from these equations are 18.7 kJ/mol for TS-1 and 25.4 kJ/mol for bismuth titanate.

Table 3 Temperature dependence of pseudo-first-order decoloration rate

Catalyst	Temperature (K)	Reaction Rate ($x10^{-3}$ min^{-1})	R^2
TS-1	288	9.35	0.99
	298	13.17	0.94
	308	15.51	0.97
BTO	288	7.84	0.98
	298	13.24	0.98
	308	15.64	0.98

R^2 is a coefficient in statistic method where $R^2 = 1$ indicates a linear relationship between the response variables and regressors while $R^2 = 0$ indicates no 'linear' relationship.

สถาบันวิทยบริการ
จุฬาลงกรณ์มหาวิทยาลัย

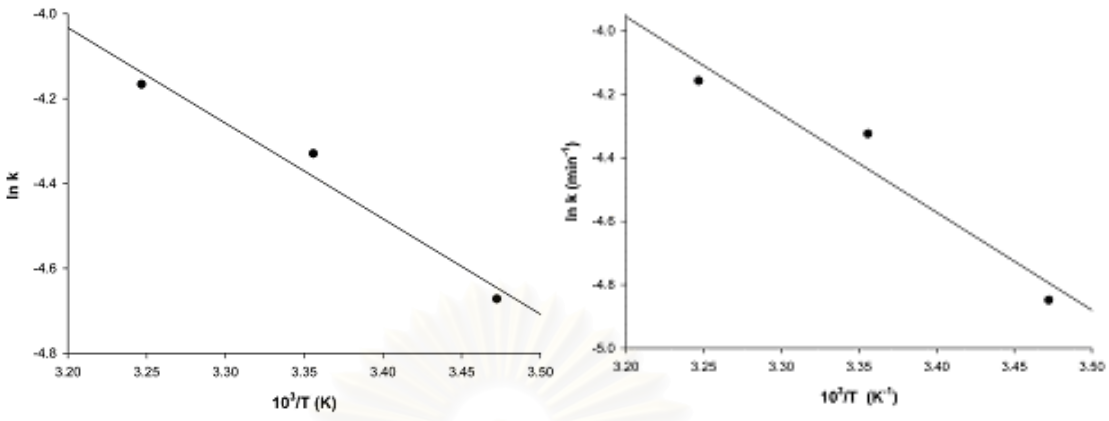

Figure 6 Activation energies of a) TS-1 and b) bismuth titanate in the presence of 30 mM of H_2O_2 at pH 3.

Comparison of TS-1 to bismuth titanate catalysts

The photocatalytic efficiency of TS-1 for decoloration and mineralization of RB5 in the presence of 30 mM H_2O_2, relative to that of bismuth titanate, is contrasted in Figure 7, which also shows data for Bi_2O_3, TiO_2, SiO_2, and in the absence of any catalyst (+30 mM H_2O_2 alone). The decoloration rate in the presence of H_2O_2 alone is the fastest in Figure 7a; it can be assumed that this reaction does not suffer from the increased turbidity associated with the presence of catalyst particles. Thus, the $^{\bullet}OH$ radicals can react with directly the dye molecules, which results in the highest rate of degradation.

สถาบันวิทยบริการ
จุฬาลงกรณ์มหาวิทยาลัย

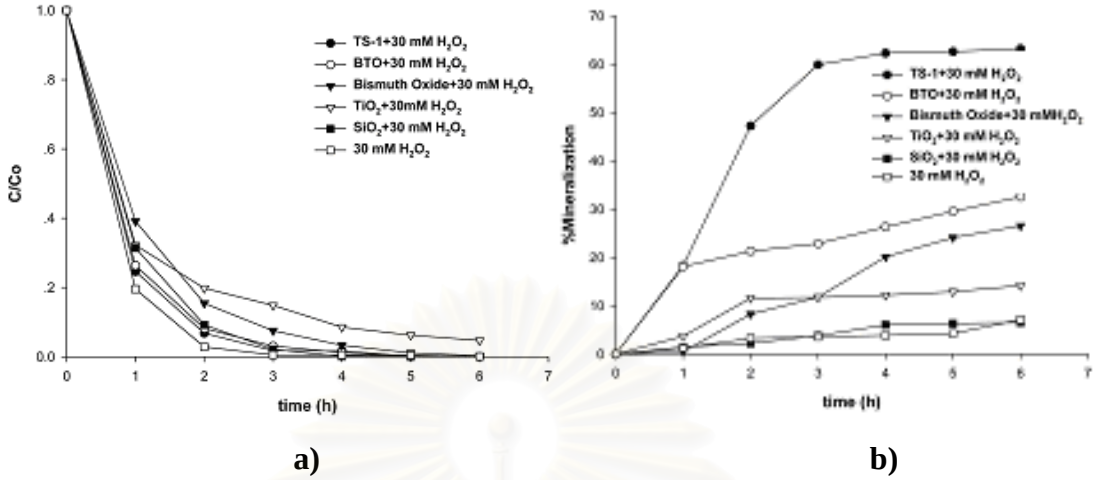

Figure 7 a) Decoloration and b) mineralization of RB5 in the presence of 30 mM H_2O_2 at pH 3 and 25°C in various systems containing TS-1 with Si/Ti = 12, bismuth titanate, bismuth oxide, TiO_2, SiO_2 and no catalyst

However, H_2O_2 alone does not degrade the dye completely to mild environmental products such a CO_2 and water, as indicated by the fact that the % mineralization remains very small (Figure 7b). To accomplish a substantial reduction in TOC of the dye, the use of a catalyst is necessary, as demonstrated in Figure 7b. In terms of TOC removal, TS-1 with Si/Ti = 12 is the most effective catalyst, when compared to the other systems.

The mechanism of degradation of each catalyst is different. The effectiveness of TS-1 depends on the amount of the reactive species titanium-hydroperoxide, whereas the catalytic action of bismuth titanate depends on the relative ease of hydroxyl radical generation and electron-hole recombination. The fact that TS-1 with high Ti content (Si/Ti = 12) in the presence of 30 mM H_2O_2 has a superior performance (65% mineralization) over bismuth titanate (30% mineralization under identical conditions) suggests that this TS-1 has large numbers of reactive centers distributed throughout the material as Ti-atoms in the zeolite framework. Moreover, since they are completely oxidized into water and CO_2 at the end of the process, it is clear that the dye molecules, as well as intermediate products, are smaller than the pore sizes of TS-1 cavities, and so can penetrate into the channels in the zeolite structure, to react with the catalytic sites [33]. E. Kusvuran et al. [34] studied the

mineralization of RB5 with wet-air oxidation and found that organic materials were not completely mineralized because of the formation of stable intermediates, such as acetic acid. However, in the presence of H_2O_2 and acetic acid, the framework titanium can form ‘framework peroxyl titanium complex’, as studied by Sooknoi et al. [35]. The framework peroxyl titanium complex is more hydrophobic than that formed by H_2O_2 alone; therefore, a stronger interaction of a non-polar substrate with the active site can be easier promoted.

The Bi-O polyhedra in bismuth titanate crystals are assumed to eliminate electron-hole recombination by oxide donors and enhance the electron transfer to O_2 [13]. However, bismuth titanate may encounter problems due to agglomeration as exhibited by other semiconductor catalysts, such as TiO_2 [9]. As the reaction proceeds, bismuth titanate particles may agglomerate and hence lose catalytically-effective surface area.

Conclusions

The photocatalytic performance of TS-1 and bismuth titanate for oxidation of RB5 was evaluated under a 6 W UV-A lamp. We observed that the catalytic efficiency of TS-1 deteriorates substantially as the pH is increased, whereas that of bismuth titanate is relatively pH insensitive. The reactivities of both TS-1 and bismuth titanate can be enhanced using high dosages of H_2O_2. The rate of decoloration was not significantly different when comparing TS-1 versus bismuth titanate, however, the degree of mineralization achieved by TS-1 with high Ti loading (Si/Ti = 12) was twice as high as bismuth titanate due to the uniform distribution of reactive Ti-centers in the zeolite framework, which enhance the reaction process. The activation energy was determined at temperatures ranging from 15-35ºC using the Arrhenius law. The activation energy of the TS-1 catalyst is 18.7 kJ/mol and the bismuth titanate 25.4 kJ/mol.

Acknowledgements

This research work is financially supported by the Postgraduate Education and Research Program in Petroleum and Petrochemical Technology (ADB) Fund

(Thailand) and the Ratchadapisake Sompote Fund, Chulalongkorn University (Thailand).

References

1. U. Pagga, D. Brown, The degradation of dyestuffs: Part II Behaviour of dyestuffs in aerobic biodegradation tests, *Chemosphere* 15 (1986) 479-491.
2. M.A. Brown, S.C. DeVito, Predicting azo dye toxicity, Crit. *Rev. Environ. Sci. Technol.* 23 (1993) 249-324.
3. E. Kusvuran, O. Gulnaz, S. Irmak, O.M. Atanur, H.I. Yavuz, O. Erbatur, Comparison of several advanced oxidation processes for the decolorization of Reactive Red 120 azo dye in aqueous solution, *J. Hazard. Mater.* B109 (2004) 85–93.
4. K. Tanaka, K. Padermpole, T. Hisanaga, Photocatalytic degradation of commercial azo dyes, *Water Res.* 34 (2000) 327–333.
5. I. Arslan, I.A. Balcioglu, D.W. Bahnemann, Advanced chemical oxidation of reactive dyes in simulated dyehouse effluents by ferrioxalate-Fenton/UV-A and TiO_2/UV-A processes, *Dyes&Pigments* 47 (2000) 207–218.
6. I.K. Konstantinou, T.A. Albanis, TiO_2-assisted photocatalytic degradation of azo dyes in aqueous solution: kinetic and mechanistic investigations: A review, *Appl. Catal. B: Environ.* 49 (2004) 1-14.
7. A. Aguedach, S. Brosilon, J. Morvan, E.K. Lhadi, Photocatalytic degradation of azo-dyes reactive black 5 and reactive yellow 145 in water over a newly deposited titanium dioxide , *Appl. Catal. B: Environ.* 57 (2005) 55-62.
8. M.R. Hoffmann, S.T. Martin, W. Choi, D.W. Bahnemann, Environmental Applications of Semiconductor Photocatalysis, *Chem. Rev.* 95 (1995) 69-96.
9. T. Torimoto, Y. Okawa, N. Takeda, H. J. Yoneyama, Effect of activated carbon content in TiO_2-loaded activated carbon on photodegradation behaviors of dichloromethane, *Photochem. Photobiol. A: Chem.* 103 (1997) 150- 157.
10. S.S. Hong, C.S. Ju, C.G. Lim, B.H. Ahn, K.T. Lim, G.D. Lee, A Photocatalytic Degradation of Phenol Over TiO2 Prepared by Sol-Gel Method *J. Ind. Eng. Chem.* 7 (2) (2001) 99-104.

11. H. Yamashita, Y. Ichihashi, M. Anpo, M. Hashimoto, C. Louis, M. Che, Photocatalytic Decomposition of NO at 275 K on Titanium Oxides Included within Y-Zeolite Cavities:The Structure and Role of the Active Sites, *J. Phys. Chem.* 100 (1996) 16041-16044.
12. M. Anpo, H. Yamashita, Y. Ichihashi, Y. Fuji, M. Honda, Photocatalytic reduction of CO_2 with H_2O on Titanium Oxides anchored within micropores of zeolites: effects of the structure of the active sites and the addition of Pt, *J. Phys. Chem.* B101 (1997) 2632.
13. V. Matjaz, S. Danilo, Processing and dielectric properties of sillenite compounds Bi[12]MO[20-δ] (M = Si, Ge, Ti, Pb, mn, B[1/2]P[1/2]) *J. Am. Ceram. Soc.* 84 (2001) 2900-2904.
14. W.F. Yao, H. Wang, X.X. Hong, X.F. Cheng, J. Huang, S.X. Shang, X.N. Yang, M. Wang, Photocatalytic property of bismuth titanate $Bi_{12}TiO_{20}$ crystals, *Appl. Catal. A: Gen.* 243 (2003) 185-190.
15. N. Phonthammachai, M. Krissanasaeranee, E. Gulari, A.M. Jamieson, S. Wongkasemjit, Crystallization and catalytic activity of high titanium loaded TS-1 zeolite, *Mat. Chem. and Phys.* 97 (2006) 458-467.
16. N. Thanabodeekij, E. Gulari, S. Wongkasemjit, $Bi_{12}TiO_{20}$ synthesized directly from bismuth (III) nitrate pentahydrate and titanium glycolate and its activity, *Powder Technology.* 160 (2005) 203-208.
17. P. Piboonchaisit, S. Wongkasemjit, R. Laine, A novel route to tris(silatranyloxy-I-propyl)amine directly from silica and triiospropanolamine, *Science-Asia J. Sci. Soc.Thailand.* 25 (1999) 113-119.
18. N. Phonthammachai, T. Chairassameewong, E. Gulari, A.M. Jamieson, S. Wongkasemjit, Oxide One Pot Synthesis of a Novel Titanium Glycolate and Its Pyrolysis, *J. Met. Mater. Min.* 12 (2002) 23.
19. C. Hachem, F. Bocquillon, O. Zahraa, M. Bouchy, Decolourization of textile industry wastewater by the photocatalytic degradation process, *Dyes&Pigments.* 49 (2001) 117-125.
20. G.D. Lee, S.K. Jung, Y.J. Jeong, J.H. Park, K.T. Lim, B.H. Ahn, S.S. Hong, Photocatalytic decomposition of 4-nitrophenol over titanium silicalite (TS-1) catalysts, *Appl. Catal. A: Gen.* 239 (2003) 197-208.

21. H. Zhan, K. Chen, H. Tian, Photocatalytic Degradation of acid azo dyes in aqueous TiO_2 suspension II. The effect of pH values, *Dyes&Pigments.* 37 (1998) 241-247.
22. G. Tozzola, M.A. Mantegazza, G. Ranghino, G. Petrini, S. Bordiag, G. Ricchiardi, C. Lamberti, R. Zulian, A. Zecchina, On the Structure of the Active Site of Ti-Silicalite in Reactions with Hydrogen Peroxide :A Vibrational and Computational Study, *J. Catal.* 179 (1998) 64-71.
23. V.N. Shetti, D. Shrinivas, P. Ratnasamy, Enhancement of chemoselectivity in epoxidation reactions over TS-1 catalysts by alkali and alkaline metal ions, *J. Molec. Catal. A: Chem.* 210 (2004) 171-178.
24. A. Houas, H. Lachheb, M. Ksibi, E. Elaloui, C. Guillard, J.M. Herrmann, Photocatalytic degradation pathway of methylene blue in water, *Appl. Catal. B: Envi.* , 31(2) (2001) 145-157.
25. P. Reeves, R. Ohlhausen, D. Sloan, K. Pamplin, T. Scoggins, C. Clark, B. Hutchinson, D.Green, Photocatalytic destruction of organic dyes in aqueous TiO_2 suspensions using concentrated simulated and natural solar energy, *Solar Energy* 48 (6) (1992) 413-420.
26. S. Naskar, S.A Pillay, M. Chanda, Photocatalytic degradation of organic dyes in aqueous solution with TiO_2 nanoparticles immobilized on foamed polyethylene sheet, *J. Photochem and Photobiol A: Chem.* 113 (3) (1998) 257-264.
27. W.F. Yao, H. Wang, X.H. Xu, X.N. Yang, Y. Zhang, S.X. Shang, M. Wang, Preparation and photocatalytic property of La (Fe)-doped bismuth titanate, *Appl. Catal. A: Gen.* 251 (2003) 235-239.
28. E. Karlsen, K. Schöffel, Titanium-silicalite catalyzed epoxidation of ethylene with hydrogen peroxide. A theoretical study, *Catal. Today.* 32 (1996) 107-114.
29. C.K. Gratzel, M. Jirousek, M. Gratzel, Decomposition of organophosphorus compounds on photoactivated TiO_2 surfaces, *J. Mol. Catal.* 60 (1990) 375-385.
30. J. Zhuang, D. Ma, Z. Yan, X. Liu, X. Han, X. Bao, Y. Zhang, X. Guo, X. Wang, Effect of acidity in TS-1 zeolites on product distribution of the styrene oxidation reaction, *Appl. Catal. A: Gen.* 258 (2004) 1-6.

31. M.S. Lucas, A.A. Dias, A. Sampaio, C. Amaral C. J.A. Peres, Degradation of a textile reactive Azo dye by a combined chemical–biological process: Fenton's reagent-yeast, *Water research* 41 (2007) 1103-1109.
32. C. Tang, V. Chen, The photocatalytic degradation of reactive black 5 using TiO_2/UV in an annular photoreactor, *Water research* 2004; 38: 2775-2781.
33. Y. Liu, X. Chen, J. Li, C. Burda, Photocatalytic degradation of azo dyes by nitrogen-doped TiO_2 nanocatalysts, *Chemosphere* 61 (2005) 11-18.
34. E. Kusvuran, S. Irmak, H.I. Yavuz, A. Samil, O. Erbatur, Comparison of the treatment methods efficiency for decolorization and mineralization of Reactive Black 5 azo dye, *J. Hazard. Mater. B* 119 (2005) 109-116.
35. T. Sooknoi, J. Limtrakul, Activity enhancement by acetic acid in cyclohexane oxidation using Ti-containing zeolite catalyst, *Appl. Cal. A: Gen.* 233 (2002) 227-237.

สถาบันวิทยบริการ
จุฬาลงกรณ์มหาวิทยาลัย